Filomat 37:13 (2023), 4351–4374
https://doi.org/10.2298/FIL2313351T

Published by Faculty of Sciences and Mathematics,
University of Niš, Serbia
Available at: http://www.pmf.ni.ac.rs/filomat

A parameter-uniform weak Galerkin finite element method for a coupled system of singularly perturbed reaction-diffusion equations

Şuayip Toprakseven[a], Peng Zhu[b]

[a]*Faculty of Engineering, Department of Computer Science, Artvin Çoruh University, Artvin, 08100, Turkey*
[b]*College of Data Science, Jiaxing University, Jiaxing, Zhejiang 314001, China*

Abstract. The aim of this paper to investigate a weak Galerkin finite element method (WG-FEM) for solving a system of coupled singularly perturbed reaction-diffusion equations. Each equation in the system has perturbation parameter of different magnitude and thus, the solutions will exhibit two distinct but overlapping boundary layers near each boundary of the domain. The proposed method is applied to the coupled system on Shishkin mesh to solve the problem theoretically and numerically. Elimination of the interior unknowns efficiently from the discrete solution system reduces the degrees of freedom and, thus the number of unknown in the discrete solution is comparable with the standard finite element scheme. The stability and error analysis of the proposed method on the Shishkin mesh are presented. We show that the method convergences of order $O(N^{-k}\ln^k N)$ in the energy norm, uniformly with respect to the perturbation parameter. Moreover, the optimal convergence rate of $O(N^{-(k+1)})$ in the L^2-norm and the superconvergence rate of $O((N^{-2k}\ln^{2k} N)$ in the discrete L^∞-norm is observed numerically. Finally, some numerical experiments are carried out to verify numerically theory.

1. Introduction

This paper deals with the following system of singularly perturbed reaction-diffusion equations: Find $\mathbf{u} = (u^1, u^2)^T \in (C^2(0,1)\cap C[0,1])^2$ such that

$$\begin{aligned} \mathcal{L}\mathbf{u} &:= -\mathcal{E}\mathbf{u}'' + \mathbf{A}\mathbf{u} = \mathbf{g} \text{ in } (0,1),\\ \mathbf{u} &= \mathbf{0} \text{ on } \{0,1\}, \end{aligned} \tag{1}$$

where the diffusion coefficients $\mathcal{E} = \mathrm{diag}(\varepsilon_1^2, \varepsilon_2^2)$ with $0 < \varepsilon_1, \varepsilon_2 << 1$ are small parameters, the vector-valued function $\mathbf{g} = (g_1, g_2)^T$ and the matrix-valued function $\mathbf{A} = (a_{kl})_{k,l=1}^2$ are twice continuously differentiable functions on $[0,1]$. We assume that $\mathbf{A} : [0,1] \to \mathbb{R}^{2\times 2}$ and the vector-valued function $\mathbf{g} : [0,1] \to \mathbb{R}^2$ are independent of $\mathcal{E}$ and the reaction matrix $\mathbf{A}$ has the following conditions

$$a_{kk} > 0, \quad a_{kl} \le 0, \quad k \ne l, \tag{2}$$

$$0 < \beta^2 < \min\{a_{11} + a_{12}, a_{21} + a_{22}\}. \tag{3}$$

2020 *Mathematics Subject Classification*. 65L10, 65L11, 65L60
Keywords. Weak Galerkin finite element method, Shishkin mesh, Coupled system of singularly perturbed problems, Uniform convergence, Stability.
Received: 24 May 2022; Revised: 12 December 2022; Accepted: 27 January 2023
Communicated by Marko Petković
Email addresses: toprakps@artvin.edu.tr (Şuayip Toprakseven), pzh@zjxu.edu.cn (Peng Zhu)

In fact, the conditions (2) and (3) imply that **A** is an **M**-matrix and its inverse is positive definite and bounded by β^{-2} in the maximum norm (see e.g., [22]). Therefore, the problem (1) has a unique solution $\mathbf{u} = (u^1, u^2)^T \in (C^2(0,1) \cap C[0,1])^2$. In general, if **g** and **A** have continuous second derivatives, the stability of $\mathcal{L}$ and the standard arguments [15], although it does not hold a maximum principle, guarantee a unique solution $\mathbf{u} \in (C^4[0,1])^2$. We assume the most general case in the rest of the paper

$$0 < \varepsilon_1 \leq \varepsilon_2 \leq 1. \tag{4}$$

The solution $\mathbf{u} = (u^1, u^2)^T$ to (1) has overlapping boundary layers both at $x = 0$ and $x = 1$ of width $O(\varepsilon_1|\ln \varepsilon_1|)$ and $O(\varepsilon_2|\ln \varepsilon_2|)$. We refer the reader to [16], [8] for further details.

Singularly perturbed problems (SPPs) are challenging differential equations to solve efficiently when the diffusion coefficient contains a very small parameter. In this case, the solution will have *boundary/interior layers* which are narrow regions near the endpoints of the domain. In these regions, the solution and its derivatives change very suddenly. The classical numerical schemes such as finite difference and finite element methods on uniform meshes produce spurious oscillation when boundary/interior layers are present, and they are inefficient and inaccurate. To overcome these inefficiencies and inaccuracies, some layer-adapted meshes have been employed for solving these type of problems. Examples of these layer-adapted meshes include Bakhvalov-type mesh [2] and Shishkin mesh [12] and they are still popular. For more discussions on layer-adapted meshes, the interested reader is referred to [22], [12], [18] and references therein.

The solution of a coupled system of singularly perturbed reaction-diffusion problems may have a sublayer when each perturbation parameter is small and of different magnitude. This renders the numerical analyses more complicated. To overcome these difficulties, a layer adapted mesh can be used in constructing a parameter-uniform numerical method for a system of coupled SPPs of reaction-diffusion type. Shishkin [23] considered a system of coupled reaction-diffusion problems on an infinite strip and it is proved that the finite difference method is robust method and has the rate of convergence $O(N^{-1/4})$ on piecewise uniform meshes when the perturbation parameters are different from each other. The standard finite difference methods with higher order convergence have been presented in [16], [14], [13] and [15] using piecewise uniform Shishkin mesh. The finite element method has been studied for SPPs in [11], [31] and [14]. Moreover, error analysis of a finite element method in a balanced norm using a quadratic splines for a linear system of coupled SPPs of reaction-diffusion type has been presented in [9]. Numerical schemes for a coupled system of SPPs of reaction-diffusion type have been presented in [3], [4], [6], [21], [7], [9] and references therein.

The WG finite element method is recently initiated and analyzed for solving partial differential equations in [32]. The main ingredient in this method is the introduction of *weak derivatives* defined on the weak function spaces and replacing the classical derivatives in the corresponding variational formulation by these weak derivatives. This replacement allows one to use completely discontinuous functions in the numerical scheme, as commonly used in discontinuous Galerkin and hybridized discontinuous Galerkin methods. However, choosing problem dependent stabilization parameters is a main concern of DG methods. Compared to DG methods, the WG-FEM is a parameter-free method in the sense that there is no need for choosing stabilization parameters and contains less unknowns. Moreover, WG-FEM is easier to implement and it has continuous normal flux across element interfaces which leads to better results with reduced degrees of freedom. By static condensation, one can eliminate the element basis functions on each local interval and results in a coupled linear system which involves only the degrees of freedom on the skeleton of the mesh. Thus, the degrees of freedom in the WG-FEM is comparable with the standard finite element method. On the other hand, the classical FEMs lack "local mass conservation" and "continuity of normal fluxes" which are two important properties of fluid dynamics. Moreover, compared with the standard FEM, the WG-FEM is flexibility in approximation scheme formulation and numerical implementation and it has possible definition on unstructured meshes and mesh adaptation, etc. The WG-FEM has been developed and employed to different types of problems such as Stokes equations [33], interface problem [20], Maxwell equation [19], time fractional convection-dominated problem [25], [28] and singularly perturbed elliptic equations in one dimension [29], [27], [26], [30] and higher dimension in [10]. Moreover, it has been shown that the method is stable and can captures accurately the boundary/interior layers for solving convection-dominated problems [10] and reaction-diffusion problems [1] while the standard Galerkin method on uniform meshes are inadequate and inefficient [22].

Motivated by the above mentioned works, we study and analyze a uniform convergence of WG-FEM for the coupled system of singularly perturbed reaction-diffusion problems (1) on piecewise uniform Shishkin mesh. The obtained result in this paper is the first uniform convergence of WG-FEM for the coupled system of singularly perturbed two-point elliptic problems in one dimension. We have proved that the proposed method is uniformly convergence of $O(N^{-1}\ln N)^k$ accurate in the discrete energy norm, where k is the order of piecewise polynomials in the weak Galerkin finite element space. Furthermore, when $\varepsilon_2 = 1$, the coupled system (1) represents the scalar fourth-order singularly perturbed problems studied in [5], thus the proposed method covers this problem as a particular case. We support numerically the theoretical results by carrying out some numerical examples.

We organize the rest of the paper as follows. A decomposition of the solution, bounds on the smooth and layer components of the solution and a piecewise uniform Shishkin mesh are given in Section 2. Section 3 introduces the WG-FEM scheme for the problem (1). The stability of the proposed method and the error estimates are analyzed in Section 4 ans Section 5, respectively. Numerous numerical examples are presented to confirm theoretical error estimates in Section 6. We remark conclusion and some future directions in the final section.

Notation. The standard Sobolev is denoted by $W^{r,p}(S)$, $H^r(S) = W^{r,2}(S)$, $H_0^1(S)$, $L^p(S) = W^{0,p}(S)$ for integers $r \geq 0$ and $p \in [1,\infty]$, and $L^2(\Omega)$ denotes the space of square integrable functions on S with the inner product $\left(\cdot,\cdot\right)_S$ for a measurable subset $S \subset \Omega$. Then, the norm $\|\cdot\|_{k,S}$ and semi-norm $|\cdot|_{k,S}$ on $H^k(S)$ are given by $\|u\|_{k,S}^2 = \sum_{j=0}^{k} \|u^{(j)}\|_{L^2(S)}^2$, $|u|_{k,S}^2 = \|u^{(k)}\|_{L^2(S)}^2$. If $S = \Omega$, we drop the subscript S.

Throughout the paper C will represent a generic positive constant which may be different but a fixed value at each location and is independent of N and the perturbation parameters ε_1, and ε_2.

2. Preliminaries

This section provides a decomposition of the solution and a priori estimates for the solution of (1) and its derivatives. This section also introduces the piecewise-uniform Shishkin mesh which is needed for a parameter uniform error analysis.

2.1. A solution decomposition

We will need the following lemma in deriving a decomposition of the solution $\mathbf{u}$.

Lemma 2.1. *[2] Let $J := [\chi, \chi+\mu]$ be an arbitrary interval with $\mu > 0$ and $r \in C^2(J)$. Then, one has*

$$\|r'\|_{L^\infty(J)} \leqslant \frac{2}{\mu}\|r\|_{L^\infty(J)} + \frac{\mu}{2}\|r''\|_{L^\infty(J)}.$$

Lemma 2.2. *Let p be a given positive integer. The solution decomposition of the solution $\boldsymbol{u}$ of the problem (1) is defined by $\boldsymbol{u} = \boldsymbol{R} + \boldsymbol{L}$ where $\boldsymbol{R} = (R^1, R^2)^T$ and $\boldsymbol{L} = (L^1, L^2)^T$ are the solutions of the following BVPs:*

$$\mathcal{L}\boldsymbol{R} = \boldsymbol{g} \quad on \quad \Omega \quad and \quad \boldsymbol{R} = \boldsymbol{A}^{-1}\boldsymbol{g} \quad on \quad \partial\Omega, \tag{5}$$

$$\mathcal{L}\boldsymbol{L} = \boldsymbol{0} \quad on \quad \Omega \quad and \quad \boldsymbol{L} = \boldsymbol{u} - \boldsymbol{R} \quad on \quad \partial\Omega. \tag{6}$$

Moreover, the solutions $\boldsymbol{R}$ and $\boldsymbol{L}$ satisfy

$$|(R^i)^{(k)}(x)| \leq C, \quad for \quad i = 1,2, \quad k = 0,1,2,\ldots,p, \tag{7}$$

$$|(L^1)^{(k)}(x)| \leq C(\varepsilon_1^{-k}\mathcal{B}_{\varepsilon_1}^{\beta}(x) + \varepsilon_2^{-k}\mathcal{B}_{\varepsilon_2}^{\beta}(x)), \quad for \quad k = 0,1,2,\ldots,p, \tag{8}$$

$$|(L^2)^{(k)}(x)| \leq C\varepsilon_2^{-k}\mathcal{B}_{\varepsilon_2}^{\beta}(x), \quad for \quad k = 0,1,2, \tag{9}$$

$$|(L^2)^{(k)}(x)| \leq C(\varepsilon_1^{-k}\mathcal{B}_{\varepsilon_1}^{\beta}(x) + \varepsilon_2^{-k}\mathcal{B}_{\varepsilon_2}^{\beta}(x)), \quad for \quad k = 3,\ldots,p, \tag{10}$$

where $\mathcal{B}_{\mu}^{\beta}(x) = e^{-\beta x/\mu} + e^{-\beta(1-x)/\mu}$ and the integer p is determined by the regularity of the solution.

Proof. The results for $k = 0, 1, 2$ are proved in [16] and [15]. We will drive the estimates for $k \geq 3$. In [16], [15], it is shown that a decomposition $\mathbf{u} = \mathbf{v} + \mathbf{w}$ satisfies the following bounds

$$|(v^i)^{(k)}(x)| \leq C, \quad for \quad i = 1, 2, \quad k = 0, 1, 2, \tag{11}$$

$$|(w^1)^{(k)}(x)| \leq C(\varepsilon_1^{-k}\mathcal{B}_{\varepsilon_1}^{\beta}(x) + \varepsilon_2^{-k}\mathcal{B}_{\varepsilon_2}^{\beta}(x)), \quad for \quad k = 0, 1, 2 \tag{12}$$

$$|(w^2)^{(k)}(x)| \leq C\varepsilon_2^{-k}\mathcal{B}_{\varepsilon_2}^{\beta}(x), \quad for \quad k = 0, 1, 2, \tag{13}$$

where $\mathbf{v} = (v^1, v^2)^T$ and $\mathbf{w} = (w^1, w^2)^T$.

We differentiate $\mathcal{L}\mathbf{v} = \mathbf{g}$ twice and find that

$$\mathcal{L}\mathbf{v}'' = \mathbf{h} := \mathbf{g}'' - \mathbf{A}''\mathbf{v} - 2\mathbf{A}'\mathbf{v}' \quad in \quad \Omega \quad and \quad \mathbf{v}''(0) = \mathbf{v}''(1) = \mathbf{0}, \tag{14}$$

We further decompose $\mathbf{v}'' = \boldsymbol{z_1} + \boldsymbol{y_1}$ as the solutions of the following boundary-value problems

$$\mathcal{L}\boldsymbol{z_1} = \mathbf{h} \quad on \quad \Omega \quad and \quad \boldsymbol{z_1} = \mathbf{A}^{-1}\mathbf{h} \quad on \quad \partial\Omega, \tag{15}$$

$$\mathcal{L}\boldsymbol{y_1} = \mathbf{0} \quad on \quad \Omega \quad and \quad \boldsymbol{y_1} = -\boldsymbol{z_1} \quad on \quad \partial\Omega. \tag{16}$$

Applying the results (11)-(13) to above decomposition, we infer that

$$|(z_1^i)^{(k)}(x)| \leq C, \quad for \quad i = 1, 2, \quad k = 0, 1, 2, \tag{17}$$

$$|(y_1^1)^{(k)}(x)| \leq C(\varepsilon_1^{-k}\mathcal{B}_{\varepsilon_1}^{\beta}(x) + \varepsilon_2^{-k}\mathcal{B}_{\varepsilon_2}^{\beta}(x)), \quad for \quad k = 0, 1, 2 \tag{18}$$

$$|(y_1^2)^{(k)}(x)| \leq C\varepsilon_2^{-k}\mathcal{B}_{\varepsilon_2}^{\beta}(x), \quad for \quad k = 0, 1, 2, \tag{19}$$

where $\boldsymbol{z_1} = (z_1^1, z_1^2)^T$ and $\boldsymbol{y_1} = (y_1^1, y_1^2)^T$. Since the operator $\mathcal{L}$ is linear, we have

$$\begin{aligned}\mathcal{L}\mathbf{u}'' &= \mathcal{L}\mathbf{v}'' + \mathcal{L}\mathbf{w}'' = \mathcal{L}\boldsymbol{z_1} + \mathcal{L}(\boldsymbol{y_1} + \mathbf{w}'') \\ &= \mathcal{L}\boldsymbol{z_1} + \mathcal{L}\mathbf{w}'',\end{aligned}$$

where we used (16).

Now, differentiating $\mathcal{L}\mathbf{w} = 0$ twice and using (12) and (13) we get

$$|(w^1)^{(k)}(x)| \leq C(\varepsilon_1^{-k}\mathcal{B}_{\varepsilon_1}^{\beta}(x) + \varepsilon_2^{-k}\mathcal{B}_{\varepsilon_2}^{\beta}(x)), \quad for \quad k = 1, 2, 4$$

$$|(w^2)^{(k)}(x)| \leq C(\varepsilon_1^{-k}\mathcal{B}_{\varepsilon_1}^{\beta}(x) + \varepsilon_2^{-k}\mathcal{B}_{\varepsilon_2}^{\beta}(x)), \quad for \quad k = 2, 4,$$

The third-order derivatives follow from Lemma 2.1 with $\mu = \varepsilon_i$ and the fact that

$$\max_{x\in I}\mathcal{B}_{\varepsilon_i}^{\beta}(x) \leqslant C\min_{x\in I}\mathcal{B}_{\varepsilon_i}^{\beta}(x) \quad \text{for any interval } I = [a, a + \varepsilon_i] \subseteq [0, 1].$$

Combining the above results, we have the following decomposition of the solution $\mathbf{u} = \mathbf{R} + \mathbf{L}$

$$\mathbf{R}^{(k)} = \begin{cases} \mathbf{v}^{(k)}, & \text{if } k = 0, 1, 2, 3, 4 \\ \boldsymbol{z_1}^{(k-2)}, & \text{if } k = 3, 4, \end{cases} \tag{20}$$

and

$$\mathbf{L}^{(k)} = \mathbf{w}^{(k)} \text{ for } k = 0, 1, 2, 3, 4. \tag{21}$$

This proves (7)-(10) for $k = 0, 1, 2, 3, 4$. Repeating the argument inductively by further decomposing $\boldsymbol{z_1}$, we get the results for $k \geq 4$. □

2.2. A piecewise uniform Shishkin mesh

We first divide the domain $\Omega = (0,1)$ into five sub-intervals as $\Omega = \sum_{s=1}^{5} \Omega_s$, where $\Omega_1 = [0,\lambda_1]$, $\Omega_2 = [\lambda_1,\lambda_2]$, $\Omega_3 = [\lambda_2, 1-\lambda_2]$, $\Omega_4 = [1-\lambda_2, 1-\lambda_1]$, $\Omega_5 = [1-\lambda_1, 1]$, respectively (see, Figure 1) where the transition points λ_1 and λ_2 are defined as

$$\lambda_1 = \min\left(\frac{1}{2}\lambda_2, \frac{(k+1)\varepsilon_1}{\beta}\ln N\right), \quad \lambda_2 = \min\left(\frac{1}{4}, \frac{(k+1)\varepsilon_2}{\beta}\ln N\right).$$

Here, k is the degree of polynomials in the approximation space and N is an integer divisible by 8. In practice, we assume $\dfrac{\lambda_2}{2} < \dfrac{(k+1)\varepsilon_1}{\beta}\ln N$; since otherwise $N^{-1} \leq \varepsilon_2$ which can be handled by using the standard arguments.

Then subdivide $[\lambda_2, 1-\lambda_2]$ into $N/2$ mesh intervals and subdivide the rest of four intervals into $N/8$ mesh intervals. An example of such a mesh with $N = 32$ is depicted in Figure 1.

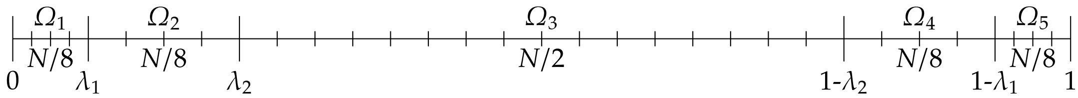

Figure 1: Piecewise-uniform Shishkin mesh with $N = 32$ for the coupled reaction-diffusion equations.

We next define the mesh points as $x_n = x_{n-1} + h_n$ with $x_0 = 0$ for $n = 1, \dots, N$ where the step size h_n given by

$$h_n = \begin{cases} h_1, & \text{for } n = 1, 2, \dots, N/8, 7N/8+1, \dots, N, \\ h_2, & \text{for } n = \frac{N}{8}+1, \dots, \frac{2N}{8}, \frac{6N}{8}+1, \dots, \frac{7N}{8}, \\ h_3, & \text{for } n = 2N/8+1, \dots, 6N/8, \end{cases}$$

with

$$h_1 = 8\lambda_1/N, \quad h_2 = 8(\lambda_2 - \lambda_1)/N, \quad h_3 = 2(1-2\lambda_2)/N.$$

Let $I_n = [x_{n-1}, x_n]$, $n = 1, \dots, N$ be the mesh and $\mathcal{T}_N = \{I_n : n = 1, \dots, N\}$ be a partition of the domain Ω. We denote $\mathbf{n}_{I_n}$ by the outward unit normal on $I_n \in \mathcal{T}_N$ and define as $\mathbf{n}_{I_n}(x_n) = 1$ and $\mathbf{n}_{I_n}(x_{n-1}) = -1$; for simplicity, we write $\mathbf{n}$ rather than $\mathbf{n}_{I_n}$.

For each element I_n, we define the broken Sobolev space by

$$H_N^k(\Omega) = \{u \in L^2(\Omega) : u|_{I_n} \in H^k(I_n), \quad \forall I_n \in \mathcal{T}_h\},$$

with the norm and semi-norm

$$\|\mathbf{u}\|^2_{H_N^k(\Omega)} = \sum_{n=1}^{N} \|u^1\|^2_{k,I_n} + \sum_{n=1}^{N} \|u^2\|^2_{k,I_n}, \quad |\mathbf{u}|^2_{H_N^k(\Omega)} = \sum_{n=1}^{N} |u^1|^2_{k,I_n} + \sum_{n=1}^{N} |u^2|^2_{k,I_n}.$$

For the sake of simplicity, we adapt the following notations.

$$\big(u,v\big) = \sum_{I_n\in\mathcal{T}_N} \big(u,v\big)_{I_n} = \sum_{I_n\in\mathcal{T}_N} \int_{I_n} u(x)v(x)\,dx, \quad \langle u,v\rangle \;\; = \sum_{I_n\in\mathcal{T}_N} \langle u,v\rangle_{\partial I_n} = \sum_{n=1}^{N} (u(x_n)v(x_n) + u(x_{n-1})v(x_{n-1})).$$

3. The WG-FEM for the coupled system of SPPs of reaction-diffusion type

This section introduces the space of weak functions and weak derivatives on this weak function space. The space of weak functions $\mathcal{F}(I_n)$ on I_n is defined as

$$\mathcal{F}(I_n) = \{u = \{u_0, u_b\} : u_0 \in L^2(I_n), u_b \text{ is the values at the endpoints of } I_n\}.$$

Here, a weak function $u = \{u_0, u_b\}$ has two components such that u_0 represents the value of u in (x_{n-1}, x_n) and u_b is not necessarily the trace of u_0. The weak function space $\mathcal{F}(I_n)$ can be embedded into the local Sobolev space $H^1(I_n)$ by the map

$$\mathcal{I}_{\mathcal{F}}(u) = \{u_0, u_b\}, \quad \forall u \in H^1(I_n), \text{ where } u_0 = u|_{I_n} \quad u_b = u|_{\partial I_n}.$$

A local WG finite element space $S_N(I_n)$ is defined for an integer $k \geq 1$ as follows:

$$S_N(I_n) = \{u = \{u_0, u_b\} : u_0|_{I_n} \in \mathbb{P}_k(I_n), u_b|_{\partial I_n} \in P_0(\partial I_n) \quad \forall I_n \in \mathcal{T}_N\}, \tag{22}$$

where $\mathbb{P}_k(I_n)$ is the set of polynomials defined on I_n of degree no more than k and $\mathbb{P}_0(\partial I_n)$ denotes constant polynomials on ∂I_n. We next define a global WG finite element space S_N consisting of weak functions $u = \{u_0, u_b\}$ such that $u_0|_{I_n} \in \mathbb{P}_k(I_n)$ and u_b is the single value at the mesh points. Let S_N^0 denote the subspace of S_N defined by

$$S_N^0 = \{u = \{u_0, u_b\} : u \in S_N, u_b(0) = u_b(1) = 0\}. \tag{23}$$

Now, the weak derivative $d_{w,I_n}u$ of a weak function $u = \{u_0, u_b\} \in S_N$ is defined as follows. For any weak function $u \in S_N(I_n)$, the **weak derivative** $d_{w,I_n}u \in \mathbb{P}_{k-1}(I_n)$ of $u = \{u_0, u_b\}$ is the unique polynomial defined on I_n satisfying the following equation

$$(d_{w,I_n}u, v)_{I_n} = -(u_0, v')_{I_n} + \langle u_b, v\mathbf{n}\rangle_{\partial I_n} \qquad \forall v \in \mathbb{P}_{k-1}(I_n), \tag{24}$$

where

$$(w, z)_{I_n} = \int_{I_n} w(x)z(x)\,dx \text{ and } \langle w, z\mathbf{n}\rangle_{\partial I_n} = w(x_n)z(x_n) - w(x_{n-1})z(x_{n-1}).$$

Then the weak derivative $d_w u$ of a weak function u on the global WG finite element space S_N is given as

$$(d_w u)|_{I_n} = d_{w,I_n}(u|_{I_n}), \quad \forall u \in S_N.$$

We now formulate the WG-FEM scheme for the system of singularly perturbed reaction-diffusion problem (1).

Algorithm 1 The WG finite element scheme for the system of SPPs of reaction-diffusion problem

1: The WG finite element approximation of the problem (1) is to seek an approximate solution $\mathbf{u}_N = (u_N^1, u_N^2) = \left(\{u_0^1, u_b^1\}, \{u_0^2, u_b^2\}\right) \in [S_N^0]^2$ satisfying

$$a(\mathbf{u}_N, \mathbf{v}_N) = L(\mathbf{v}_N), \quad \forall \mathbf{v}_N = (v_N^1, v_N^2) \in [S_N^0]^2, \tag{25}$$

where the bilinear form $a(\mathbf{u}_N, \mathbf{v}_N) = a_1(\mathbf{u}_N, \mathbf{v}_N) + a_2(\mathbf{u}_N, \mathbf{v}_N)$ and the linear form $L(\mathbf{v}_N)$ are defined as follows: for any $\mathbf{u}_N = (u_N^1, u_N^2) = \left(\{u_0^1, u_b^1\}, \{u_0^2, u_b^2\}\right), \mathbf{v}_N = (v_N^1, v_N^2) = \left(\{v_0^1, v_b^1\}, \{v_0^2, v_b^2\}\right) \in [S_N]^2$

$$a_1(\mathbf{u}_N, \mathbf{v}_N) = \varepsilon_1^2(d_w u_N^1, d_w v_N^1) + s(u_N^1, v_N^1) + \left(a_{11}u_0^1 + a_{12}u_0^2, v_0^1\right), \tag{26}$$

$$a_2(\mathbf{u}_N, \mathbf{v}_N) = \varepsilon_2^2(d_w u_N^2, d_w v_N^2) + s(u_N^2, v_N^2) + \left(a_{21}u_0^1 + a_{22}u_0^2, v_0^2\right), \tag{27}$$

$$s(u_N^\ell, v_N^\ell) = \sum_{n=1}^{N} \langle \sigma_n(u_0^\ell - u_b^\ell), v_0^\ell - v_b^\ell \rangle_{\partial I_n}, \quad \ell = 1, 2,$$
$$L(\mathbf{v}_N) = (g_1, v_0^1) + (g_2, v_0^2),$$

where $\sigma_n \geq 0$, $n = 1, \dots N$ is the penalization parameter associated with the node x_n defined as follows:

$$\sigma_n = \begin{cases} 1, & \text{for } I_n \subset \Omega_3 \\ \dfrac{N}{\ln N}, & \text{for } I_n \subset \Omega \setminus \Omega_3. \end{cases} \tag{28}$$

The penalty parameter is crucial in the uniform convergence estimates. Usually, the penalty parameter is chosen as $\sigma_n = \varepsilon_2^2 h_n^{-1}$ in the WG finite element schemes [10, 32, 33]. However, this choice is inappropriate for our uniform convergence analysis. In [35], Zhang and Liu proposed a WG-FEM for convection-dominated problem on Bakhvalov-type mesh and they proved the uniform convergence results by defining two different penalty terms, which are

$$\sigma_n = \begin{cases} 1 & \text{for } n = N/2 - 1, \\ \varepsilon h_n^{-1} & \text{otherwise} \end{cases} \text{ and } \sigma_n = \begin{cases} 1 & \text{for } n \geqslant N/2 - 1 \\ \varepsilon h_n^{-1} & \text{otherwise} \end{cases}.$$

The authors presented a uniform convergent WG-FEM on Shishkin mesh for convection-dominated problem in $2D$ using the penalty parameter similar to our penalty term (28) in [34].

4. Stability of the numerical scheme

We will use the following trace inequalities in the analysis.

$$\|v\|_{L^2(\partial I_n)}^2 \leq C(h_n^{-1}\|v\|_{L^2(I_n)}^2 + \|v\|_{L^2(I_n)}\|v'\|_{L^2(I_n)}), \quad \forall v \in H^1(I_n), \tag{29}$$

$$\|v_N\|_{L^p(\partial I_n)} \leq C h_n^{-1/p}\|v_N\|_{L^p(I_n)}, \quad \forall 1 \leq p \leq \infty, \forall v_N \in \mathbb{P}_k(I_n). \tag{30}$$

We introduce the $(\varepsilon_1, \varepsilon_2)-$ weighted energy norm $|||\cdot|||$ in $[S_N]^2$ as follows: for $\mathbf{v} = (v_N^1, v_N^2) = \left(\{v_0^1, v_b^1\}, \{v_0^2, v_b^2\}\right) \in [S_N]^2$,

$$|||\mathbf{v}|||^2 = \varepsilon_1^2\|d_w v_N^1\|^2 + \varepsilon_2^2\|d_w v_N^2\|^2 + \beta^2(\|v_0^1\|^2 + \|v_0^2\|^2) + s(v_N^1, v_N^1) + s(v_N^2, v_N^2). \tag{31}$$

The discrete H^1 energy-like norm $|||\cdot|||_\varepsilon$ in $[S_N]^2 + [H_0^1(\Omega)]^2$ is given by

$$|||\mathbf{v}|||_\varepsilon^2 = \varepsilon_1^2\|Dv_0^1\|^2 + \varepsilon_2^2\|Dv_0^2\|^2 + \beta^2(\|v_0^1\|^2 + \|v_0^2\|^2) + s(v_N^1, v_N^1) + s(v_N^2, v_N^2), \tag{32}$$

where $Dw := \dfrac{dw}{dx}$ which sometimes denoted by w' is the ordinary derivative of a function $w(x)$.

We point out that a function $w \in H_0^1(\Omega)$ can be interpreted as a weak function $w = \{w_0, w_b\}$ with $w_0 = w|_{I_n}$ and $w_b = w|_{\partial I_n}$ for I_n.

We show that the norms $|||\cdot|||$ and $|||\cdot|||_\varepsilon$ defined by (31) and (32), respectively are equivalent in the WG finite element space $[S_N^0]^2$ in the next lemma.

Lemma 4.1. *Let $\boldsymbol{v}_N = (v_N^1, v_N^2) \in [S_N^0]^2$. Then there exists a constant C such that*

$$C|||\boldsymbol{v}_N||| \le |||\boldsymbol{v}_N|||_\varepsilon \le C|||\boldsymbol{v}_N|||. \tag{33}$$

Proof. For $v_N^1 = \{v_0^1, v_b^1\} \in S_N^0$, it follows from the definition of weak derivative (24) and integration by parts that

$$\left(d_w v_N^1, w\right)_{I_n} = \left(Dv_0^1, w\right)_{I_n} + \langle v_b^1 - v_0^1, w\mathbf{n}\rangle_{\partial I_n}, \quad \forall w \in \mathbb{P}_{k-1}(I_n). \tag{34}$$

Choosing $w = d_w v_N^1$ in the above equation (34) yields

$$\|d_w v_N^1\|_{I_n}^2 = \left(Dv_0^1, d_w v_N^1\right)_{I_n} + \langle v_b^1 - v_0^1, d_w v_N^1 \mathbf{n}\rangle_{\partial I_n}.$$

Using the Cauchy-Schwarz inequality and the trace inequality (30) reveals that

$$\begin{aligned} \|d_w v_N^1\|_{I_n}^2 &= \|Dv_0^1\|_{I_n} \|d_w v_N^1\|_{I_n} + \|v_b^1 - v_0^1\|_{\partial I_n} \|d_w v_N^1\|_{\partial I_n} \\ &\le \left(\|Dv_0^1\|_{I_n} + Ch_n^{-1/2}\|v_b^1 - v_0^1\|_{\partial I_n}\right)\|d_w v_N^1\|_{I_n}. \end{aligned}$$

Therefore, we have

$$\|d_w v_N^1\|_{I_n} \le \|Dv_0^1\|_{I_n} + Ch_n^{-1/2}\|v_b^1 - v_0^1\|_{\partial I_n}.$$

Squaring and then summing over the mesh $I_n \in \mathcal{T}_h$ gives that

$$\varepsilon_1^2\|d_w v_N^1\|^2 \le 2\Big(\varepsilon_1^2\|Dv_0^1\|^2 + C\sum_{n=1}^{N} \varepsilon_1^2 h_n^{-1}\|v_b^1 - v_0^1\|_{\partial I_n}^2\Big). \tag{35}$$

From the penalty parameter (28), we have

$$\frac{\varepsilon_\ell^2 h_n^{-1}}{\sigma_n} \le C, \quad \ell = 1, 2, \quad \textit{for } n = 1, \dots, N. \tag{36}$$

Hence using (36), we obtain

$$\sum_{n=1}^{N} \varepsilon_1^2 h_n^{-1}\|v_b^1 - v_0^1\|_{\partial I_n}^2 = \sum_{n=1}^{N} \frac{\varepsilon_1^2 h_n^{-1}}{\sigma_n}\sigma_n\|v_b^1 - v_0^1\|_{\partial I_n}^2 \le Cs(v_N^1, v_N^1)$$

which together with (35) implies that

$$\varepsilon_1^2\|d_w v_N^1\|^2 \le 2\Big(\varepsilon_1^2\|Dv_0^1\|^2 + s(v_N^1, v_N^1)\Big). \tag{37}$$

Using again (36), one can drive the same result for $v_N^2 \in S_N^0$ as follows

$$\varepsilon_2^2\|d_w v_N^2\|^2 \le 2\Big(\varepsilon_2^2\|Dv_0^2\|^2 + Cs(v_N^2, v_N^2)\Big). \tag{38}$$

On the other hand, taking $w = Dv_0^1$ in the equation (34) yields

$$\|Dv_0^1\|_{I_n}^2 = \left(Dv_0^1, d_w v_N^1\right)_{I_n} - \langle v_b^1 - v_0^1, Dv_0^1\mathbf{n}\rangle_{\partial I_n}.$$

Using the Cauchy-Schwarz inequality and the trace inequality (30), we arrive at

$$\begin{aligned} \|Dv_0^1\|_{I_n}^2 &\le \|d_w v_N^1\|_{I_n}\|Dv_0^1\|_{I_n} + \|v_b^1 - v_0^1\|_{\partial I_n}\|Dv_0^1\|_{\partial I_n} \\ &\le \left(\|d_w v_N^1\|_{I_n} + Ch_n^{-1/2}\|v_b^1 - v_0^1\|_{\partial I_n}\right)\|Dv_0^1\|_{I_n}. \end{aligned}$$

Therefore, we obtain

$$\|Dv_0^1\|_{I_n} \le \|d_w v_N^1\|_{I_n} + Ch_n^{-1/2}\|v_b^1 - v_0^1\|_{\partial I_n}.$$

With the help of (36) we result in

$$\varepsilon_1^2\|Dv_0^1\|_{I_n}^2 \le 2\Big(\varepsilon_1^2\|d_w v_N^1\|^2 + Cs(v_N^1, v_N^1)\Big). \tag{39}$$

One can show the same result for v_N^2 as follows

$$\varepsilon_2^2\|Dv_0^2\|_{I_n}^2 \le 2\Big(\varepsilon_2^2\|d_w v_N^2\|^2 + Cs(v_N^2, v_N^2)\Big). \tag{40}$$

Using the inequalities (37)-(38) and (39)-(40) and considering the definition of the norms $|||\cdot|||$ and $|||\cdot|||_\varepsilon$, the desired result (33) follows immediately. This completes the proof. □

The bilinear form $a(\cdot,\cdot)$ given by (25) is coercive as shown in the next lemma.

Lemma 4.2. *Let $v_N = \Big(\{v_0^1, v_b^1\}, \{v_0^2, v_b^2\}\Big) \in [S_N^0]^2$. Then there exists a constant C such that*

$$a(v_N, v_N) \ge |||v_N|||^2. \tag{41}$$

Proof. The assumption (3) on the reaction matrix $\mathbf{A}$ implies that for any $x \in \Omega$

$$\mathbf{z}^T\mathbf{A}\mathbf{z} \ge \beta^2\mathbf{z}^T\mathbf{z}, \quad \forall \mathbf{z} \in \mathbb{R}^2.$$

It follows from the above fact that for any $\mathbf{v}_N = (v_N^1, v_N^2) = \Big(\{v_0^1, v_b^1\}, \{v_0^2, v_b^2\}\Big)$

$$\begin{aligned}
a(\mathbf{v}_N, \mathbf{v}_N) &= \varepsilon_1^2\|d_w v_N^1\|^2 + s(v_N^1, v_N^1) + \Big(a_{11}v_0^1 + a_{12}v_0^2, v_0^1\Big) \\
&\quad + \varepsilon_2^2\|d_w v_N^2\|^2 + s(v_N^2, v_N^2) + \Big(a_{21}v_0^1 + a_{22}v_0^2, v_0^2\Big) \\
&\ge \varepsilon_1^2\|d_w v_N^1\|^2 + s(v_N^1, v_N^1) + \varepsilon_2^2\|d_w v_N^2\|^2 + s(v_N^2, v_N^2) + \beta^2(\|v_0^1\|^2 + \|v_0^2\|^2) \\
&= |||\mathbf{v}_N|||^2,
\end{aligned}$$

where β is given by (3). The proof is completed. □

In light of Lemma 4.2, we deduce that

$$|||\mathbf{u}_N||| \le \|\mathbf{g}\|.$$

This stability estimate shows that the problem (1) has a unique solution which implies the existence of the solution. As a result of Lemma 4.1 and Lemma 4.2, we conclude that the bilinear form $a(\cdot,\cdot)$ is also coercive in the energy like norm $|||\cdot|||_\varepsilon$ defined by (32).

Lemma 4.3. *Let $v_N = \Big(\{v_0^1, v_b^1\}, \{v_0^2, v_b^2\}\Big) \in [S_N^0]^2$. Then there exists a constant C such that*

$$a(v_N, v_N) \ge C|||v_N|||_\varepsilon^2. \tag{42}$$

5. Error estimates

This section aims to present an error analysis of the WG-FEM for solving the problem (1). Robust uniform convergent WG-FEM on the piecewise Shishkin mesh is developed. We will use a special interpolation operator introduced in [31] in the following analyses. On each interval I_n, we introduce the set of $k+1$ nodal functional N_m defined as follows: for any $v \in C(I_n)$

$$N_0(v) = v(x_{n-1}), \quad N_k(v) = v(x_n),$$
$$N_m(v) = \frac{1}{h_n^m} \int_{x_{n-1}}^{x_n} (x - x_{n-1})^{m-1} v(x)\, dx, \quad m = 1, \dots, k-1.$$

A local interpolation $\mathcal{I} : H^1(I_n) \to \mathbb{P}_k(I_n)$ is now defined by

$$N_m(\mathcal{I}v - v) = 0, \quad m = 0, 1, \dots, k. \tag{43}$$

A continuous global interpolation can be constructed from the local interpolation operator $\mathcal{I}$.

For simplicity, we denote $\mathcal{I}v|_{\partial I_n}$ again by $\mathcal{I}v|_{I_n}$ since $\mathcal{I}v|_{I_n}$ is continuous on I_n. Note that for any $v \in H^1(I_n)$ we have

$$d_w(\mathcal{I}v) = (\mathcal{I}v)'. \tag{44}$$

Lemma 5.1. *[31] For any $w \in H^{k+1}(I_n), I_n \in \mathcal{T}_N$, the interpolation $\mathcal{I}w$ defined by (43) has the following estimates:*

$$|w - \mathcal{I}w|_{l,I_n} \le C h_n^{k+1-l} |w|_{k+1,I_n}, \quad l = 0, 1, \dots, k+1, \tag{45}$$
$$\|w - \mathcal{I}w\|_{L_\infty(I_n)} \le C h_n^{k+1} |w|_{k+1,\infty,I_n}, \tag{46}$$

where h_n is the length of element I_n and C is independent of h_n, ε_1 and ε_2.

Lemma 5.2. *Let $\mathcal{I}\boldsymbol{R}$ and $\mathcal{I}\boldsymbol{L}$ be the interpolations of the regular part $\boldsymbol{R}$ and the layer part $\boldsymbol{L}$ of the solution on the piecewise-uniform Shishkin mesh, respectively. Assume that $\varepsilon_2 \ln N \le \beta/4(k+1)$. Then, we have $\mathcal{I}\boldsymbol{u} = \mathcal{I}\boldsymbol{R} + \mathcal{I}\boldsymbol{L}$ and the following interpolation estimates are satisfied for $\ell = 1, 2$:*

$$\|u^\ell - \mathcal{I}u^\ell\|_{L^\infty(\Omega_s)} \le C(N^{-1}\ln N)^{k+1}, \quad s = 1, 2, 4, 5, \tag{47}$$
$$\|u^\ell - \mathcal{I}u^\ell\|_{L^\infty(\Omega_3)} \le CN^{-(k+1)}, \tag{48}$$
$$\|(R^\ell - \mathcal{I}R^\ell)^{(p)}\|_{L^2(\Omega)} \le CN^{l-(k+1)}, \ p = 0, \dots, k, \tag{49}$$
$$\|L^\ell - \mathcal{I}L^\ell\|_{L^2(\Omega_s)} \le C\varepsilon_2^{1/2}(N^{-1}\ln N)^{k+1}, \quad s = 1, 2, 4, 5, \tag{50}$$
$$N^{-1}\|(\mathcal{I}L^\ell)'\|_{L^2(\Omega_3)} + \|\mathcal{I}L^\ell\|_{L^2(\Omega_3)} \le C(\varepsilon_2^{1/2} + N^{-1/2})N^{-(k+1)}, \tag{51}$$
$$\|L^\ell\|_{L^\infty(\Omega_3)} + \varepsilon_2^{-1/2}\|L^\ell\|_{L^2(\Omega_3)} \le CN^{-(k+1)}, \tag{52}$$
$$\|(L^\ell)^{(l)}\|_{L^2(\Omega_3)} \le C\varepsilon_2^{1/2-l}N^{-(k+1)}. \tag{53}$$

If $u^\ell \in H^{k+1}(\Omega)$ for $\ell = 1, 2$, we also have

$$\|(L^\ell - \mathcal{I}L^\ell)^{(l)}\|_{L^2(\Omega_3)} \le C\varepsilon_2^{1/2-l}N^{-(k+1)}, \quad l = 1, 2, \tag{54}$$
$$\|(L^\ell - \mathcal{I}L^\ell)^{(l)}\|_{L^2(\Omega_s)} \le C\varepsilon_2^{1/2-l}(N^{-1}\ln N)^{k+1-p}, \quad p = 1, 2, \quad s = 1, 2, 4, 5. \tag{55}$$

Proof. The fact $\mathcal{I}\mathbf{u} = \mathcal{I}(\mathbf{R} + \mathbf{L}) = \mathcal{I}\mathbf{R} + \mathcal{I}\mathbf{L}$ follows from the linearity of the interpolation. From the estimate (46), one has

$$\|u^\ell - \mathcal{I}u^\ell\|_{L^\infty(\Omega_s)} \le Ch_n^{k+1}|(u^\ell)^{(k+1)}|_{L^\infty(\Omega_s)}, \quad \ell = 1, 2. \tag{56}$$

Using the regularity of the solution and the bounds on the regular and the layer parts of the solution given in Lemma 2.2, one can show that

$$|(u^1)^{(k+1)}|_{L^\infty(\Omega_s)} \le |(R^1)^{(k+1)}|_{L^\infty(\Omega_s)} + |(L^1)^{(k+1)}|_{L^\infty(\Omega_s)} \le C\Big(\varepsilon_1^{-(k+1)}\mathcal{B}^{\beta}_{\varepsilon_1}(x) + \varepsilon_2^{-(k+1)}\mathcal{B}^{\beta}_{\varepsilon_2}(x)\Big).$$

Since $h_n = h_1 = 8\lambda_1/N = \dfrac{8(k+1)\varepsilon_1}{\beta}N^{-1}\ln N$ on the sub-intervals Ω_1 and Ω_5, the estimate (56) implies that

$$\|u^1 - \mathcal{I}u^1\|_{L^\infty(\Omega_s)} \le C(N^{-1}\ln N)^{k+1}, \quad s = 1, 5.$$

Knowing that $h_n = h_2 = 8(\lambda_2-\lambda_1)/N = \dfrac{8(k+1)(\varepsilon_2-\varepsilon_1)}{\beta}N^{-1}\ln N$ on the sub-intervals Ω_2 and Ω_4 we similarly obtain from (56)

$$\|u^1 - \mathcal{I}u^1\|_{L^\infty(\Omega_s)} \le C(N^{-1}\ln N)^{k+1}, \quad s = 2, 4.$$

By using Lemma 2.2, one can show that the second component u^2 of the solution has the estimate

$$|(u^2)^{(k+1)}|_{L^\infty(\Omega_s)} \le C\varepsilon_2^{-(k+1)}|\mathcal{B}^{\beta}_{\varepsilon_2}(x)|.$$

This inequality and the estimate (56) conclude that

$$\|u^2 - \mathcal{I}u^2\|_{L^\infty(\Omega_s)} \le C(N^{-1}\ln N)^{k+1}, \quad s = 1, 2, 4, 5.$$

Thus, the estimate (47) is now proved.

Using the interpolation estimate (45) and Lemma 2.2 on the regular component $\mathbf{R}$ of the solution, we obtain

$$\|(R^\ell - \mathcal{I}R^\ell)^{(l)}\|_{L^2(\Omega)} \le CN^{l-(k+1)}|R^\ell|_{k+1,I_n} \le CN^{l-(k+1)} \quad l = 0, 1 \dots, k.$$

This completes the proof of the estimate (49).

Using the fact that $\mathcal{B}^{\beta}_{\varepsilon_1}(x) \le \mathcal{B}^{\beta}_{\varepsilon_2}(x)$ and $\lambda_2 = \dfrac{(k+1)\varepsilon_2}{\beta}\ln N$, we have

$$\begin{aligned}\|L^\ell\|_{L^\infty(\Omega_3)} &\le C\max_{[\lambda_2,1-\lambda_2]}\Big(\mathcal{B}^{\beta}_{\varepsilon_1}(x) + \mathcal{B}^{\beta}_{\varepsilon_2}(x)\Big)\\ &\le C\max_{[\lambda_2,1-\lambda_2]}\Big(\exp(-\beta x/\varepsilon_2) + \exp(-\beta(1-x)/\varepsilon_2)\Big)\\ &\le CN^{-(k+1)}.\end{aligned}$$

The L^2- norm estimate of the layer part of the solution on the sub-interval Ω_3 follows from

$$\begin{aligned}\|L^\ell\|^2_{L^2(\Omega_3)} &\le C\int_{\lambda_2}^{1-\lambda_2}\Big(\mathcal{B}^{\beta}_{\varepsilon_1}(x) + \mathcal{B}^{\beta}_{\varepsilon_2}(x)\Big)^2 dx\\ &\le C\int_{\lambda_2}^{1-\lambda_2}\Big(\exp(-2\beta x/\varepsilon_2) + \exp(-2\beta(1-x)/\varepsilon_2)\Big)dx\\ &\le C\varepsilon_2 N^{-2(k+1)}.\end{aligned}$$

Therefore, we have

$$\|L^\ell\|_{L^\infty(\Omega_3)} + \varepsilon_2^{-1/2}\|L^\ell\|_{L^2(\Omega_3)} \le CN^{-(k+1)}.$$

Thus, we complete the proof of the estimate (52).

Using the fact that

$$\varepsilon_1^{-k}\mathcal{B}_{\varepsilon_1}^{\beta}(x) \le \varepsilon_2^{-k}\mathcal{B}_{\varepsilon_2}^{\beta}(x), \tag{57}$$

we obtain at once

$$\begin{aligned}\|(L^{\ell})^{(l)}\|^2_{L^2(\Omega_3)} &\le C\int_{\lambda_2}^{1-\lambda_2}\Big((\mathcal{B}_{\varepsilon_1}^{\beta}(x)+\mathcal{B}_{\varepsilon_2}^{\beta}(x))^{(l)}\Big)^2 dx\\ &\le C\varepsilon_2^{-2l}\int_{\lambda_2}^{1-\lambda_2}\Big(\exp(-2\beta x/\varepsilon_2)+\exp(-2\beta(1-x)/\varepsilon_2)\Big)dx\\ &\le C\varepsilon_2^{1-2l}N^{-2(k+1)}.\end{aligned}$$

This proves the estimate (53).

Due to (45) of Lemma 5.1, (8)-(10) and the above fact (57), we obtain

$$\begin{aligned}\|L^{\ell}-\mathcal{I}L^{\ell}\|^2_{L^2(\Omega_s)} &= \sum_{I_n\subset\Omega_s}\|L^{\ell}-\mathcal{I}L^{\ell}\|^2_{L^2(I_n)}\\ &\le Ch_1^{2(k+1)}\Big(\int_0^{\lambda_1}\Big(\mathcal{B}_{\varepsilon_1}^{\beta}(x)+\mathcal{B}_{\varepsilon_2}^{\beta}(x)\Big)^2dx+\int_{1-\lambda_1}^{1}\Big(\mathcal{B}_{\varepsilon_1}^{\beta}(x)+\mathcal{B}_{\varepsilon_2}^{\beta}(x)\Big)^2dx\Big)\\ &\le C\varepsilon_2(N^{-1}\ln N)^{2(k+1)} \quad \textit{for} \quad s=1,4.\end{aligned}$$

Similarly one can show that the above estimate holds on the sub-intervals Ω_s, $s = 2, 5$. Thus, the estimate (50) is proved.

For the proof of (51) we follow [31]. An inverse estimate yields that

$$N^{-1}\|(\mathcal{I}L^{\ell})'\|_{L^2(\Omega_3)} \le C\|\mathcal{I}L^{\ell}\|_{L^2(\Omega_3)}.$$

We will derive a bound for $\|\mathcal{I}L^{\ell}\|_{L^2(\Omega_3)}$. For the interval $I_n = (x_{n-1}, x_n)$, we have the estimate for the local nodal functional $N_m(L^{\ell})$ as

$$|N_m(L^{\ell})| \le C\Big(\exp(-\beta x_{n-1}/\varepsilon_2)+\exp(-\beta(1-x_n)/\varepsilon_2)\Big).$$

The local representation

$$\mathcal{I}L^{\ell}|_{I_n} = \sum_{m=0}^{k} N_m(L^{\ell})\phi_m$$

implies that

$$\begin{aligned}\|\mathcal{I}L^{\ell}\|^2_{L^2(I_n)} &\le \sum_{m=0}^{k}|N_m(L^{\ell})|^2\|\phi_m\|^2_{L^2(I_n)}\\ &\le CN^{-1}\Big(\exp(-2\beta x_{n-1}/\varepsilon_2)+\exp(-2\beta(1-x_n)/\varepsilon_2)\Big),\end{aligned} \tag{58}$$

where we use the fact $\|\phi_m\|_{L^2(I_n)} \le CN^{-1}$. Summing up over all $I_n \subset \Omega_3$ yields that

$$\sum_{n=2N/8+1}^{6N/8}\|\mathcal{I}L^{\ell}\|^2_{L^2(I_n)} \le CN^{-1}\sum_{n=2N/8+1}^{6N/8}\Big(\exp(-2\beta x_{n-1}/\varepsilon_2)+\exp(-2\beta(1-x_n)/\varepsilon_2)\Big).$$

Since the mesh size on Ω_3 is h_3, the term in the parenthesis on the right hand side of the above inequality can be written as

$$\begin{aligned}&\exp(-2\beta x_{n-1}/\varepsilon_2)+\exp(-2\beta(1-x_n)/\varepsilon_2)\\ =&\exp((-2\beta x_{n-1}+2\beta x_n-2\beta x_n)/\varepsilon_2)+\exp((-2\beta(1-x_n)+2\beta x_{n-1}-2\beta x_{n-1})/\varepsilon_2)\\ \le&\exp(2h_3\beta/\varepsilon_2)\Big(\exp(-2\beta x/\varepsilon_2)+\exp(-2\beta(1-x)/\varepsilon_2)\Big),\quad \textit{for}\quad x_{n-1}<x<x_n.\end{aligned}$$

Integrating the above inequality on $I_n\subset\Omega_3$ and using the fact that $\frac{1}{N}\le h_3\le\frac{2}{N}$, we have

$$\begin{aligned}&N^{-1}\Big(\exp(-2\beta x_{n-1}/\varepsilon_2)+\exp(-2\beta(1-x_n)/\varepsilon_2)\Big)\\ \le&\exp(2h_3\beta/\varepsilon_2)\int_{x_{n-1}}^{x_n}\Big(\exp(-2\beta x/\varepsilon_2)+\exp(-2\beta(1-x)/\varepsilon_2)\Big)dx.\end{aligned}$$

Summing up the above inequality for $n=2N/8+1,\dots,6N/8-1$ leads to

$$\begin{aligned}&N^{-1}\sum_{n=2N/8+1}^{6N/8-1}\Big(\exp(-2\beta x_{n-1}/\varepsilon_2)+\exp(-2\beta(1-x_n)/\varepsilon_2)\Big)\\ \le&\exp(2h_3\beta/\varepsilon_2)\int_{x_{2N/8}}^{x_{6N/8-1}}\Big(\exp(-2\beta x/\varepsilon_2)+\exp(-2\beta(1-x)/\varepsilon_2)\Big)dx\\ \le& C\varepsilon_2N^{-2(k+1)}.\end{aligned}$$

It remains to bound on the last interval $(x_{6N/8-1},x_{6N/8})$. From the estimate (58), we have

$$\begin{aligned}\|\mathcal{I}L^\ell\|^2_{L^2(I_{6N/8})}&\le N^{-1}\Big(\exp(-2\beta x_{6N/8-1}/\varepsilon_2)+\exp(-2\beta(1-x_{6N/8})/\varepsilon_2)\Big)\\ &\le CN^{-(1+2(k+1))}.\end{aligned}$$

These two last estimates give the desired estimate. Thus the estimate (51) is proved.

We now prove the estimate (48). It follows from the local representation of $\mathcal{I}L^\ell|_{I_n}$ that

$$\|\mathcal{I}L^\ell\|_{L^\infty(I_n)}\le\sum_{m=0}^{k}|N_m(L^\ell)|\|\phi_m\|_{L^\infty(I_n)}\le CN^{-(k+1)},\quad\forall I_n\subset\Omega_3.$$

Using Lemma 5.1 and the estimate (52) we have

$$\|u^\ell-\mathcal{I}u^\ell\|_{L^\infty(\Omega_3)}\le\|R^\ell-\mathcal{I}R^\ell\|_{L^\infty(\Omega_3)}+\|L^\ell\|_{L^\infty(\Omega_3)}+\|\mathcal{I}L^\ell\|_{L^\infty(\Omega_3)}\le CN^{-(k+1)},$$

which proves the estimate (48). The proofs of (54) and (55) are similar the ones given in [36]. Thus we complete the proof of the lemma. □

Since the exact solution of problem (1) does not satisfy the WG-FEM scheme (25), the WG-FEM is inconsistent. Because of this property of the method, the classical Galerkin orthogonality is lost. Consequently we will have a consistency error in the error analysis. We first obtain error equations which help to derive the consistency error in the error analysis.

Lemma 5.3. *Let $\boldsymbol{u}=(u^1,u^2)$ be the solution of the problem (1). Then for any $\boldsymbol{v}_N=(v_N^1,v_N^2)=\Big(\{v_0^1,v_b^1\},\{v_0^2,v_b^2\}\Big)\in[S_N^0]^2$, we have*

$$-\varepsilon_\ell^2\Big((u^\ell)'',v_0^\ell\Big)=\varepsilon_\ell^2\Big(d_w(\mathcal{I}u^\ell),d_wv_N^\ell\Big)-T_1(u^\ell,v_N^\ell),\quad \ell=1,2,\tag{59}$$

$$\Big(a_{11}u^1+a_{12}u^2,v_0^1\Big)+\Big(a_{21}u^1+a_{22}u^2,v_0^2\Big)=\Big(a_{11}\mathcal{I}u^1+a_{12}\mathcal{I}u^2,v_0^1\Big)+\Big(a_{21}\mathcal{I}u^1+a_{22}\mathcal{I}u^2,v_0^2\Big)-T_2(\boldsymbol{u},\boldsymbol{v}_N),\tag{60}$$

where

$$T_1(u^\ell, v_N^\ell) = \varepsilon_\ell^2 \langle (u^\ell - \mathcal{I}u^\ell)', \boldsymbol{n}(v_0^\ell - v_b^\ell)\rangle, \quad \ell = 1,2, \tag{61}$$

$$T_2(\boldsymbol{u}, \boldsymbol{v}_N) = \left(a_{11}(\mathcal{I}u^1 - u^1) + a_{12}(\mathcal{I}u^2 - u^2), v_0^1\right) + \left(a_{21}(\mathcal{I}u^1 - u^1) + a_{22}(\mathcal{I}u^2 - u^2), v_0^2\right). \tag{62}$$

Proof. For any $\mathbf{v}_N \in [S_N^0]^2$, with the aid of the commutative property (44) of the interpolation operator we have

$$\left(d_w(\mathcal{I}u^\ell), d_w v_N^\ell\right)_{I_n} = \left((\mathcal{I}u^\ell)', d_w v_N^\ell\right)_{I_n}, \quad \ell = 1,2, \quad \forall I_n \in \mathcal{T}_h. \tag{63}$$

By using the definition of the weak derivative (24) and integration by parts, one has

$$\begin{aligned} \left(d_w v_N^\ell, (\mathcal{I}u^\ell)'\right)_{I_n} &= -\left(v_N^\ell, (\mathcal{I}u^\ell)''\right)_{I_n} + \langle (\mathcal{I}u^\ell)', \mathbf{n} v_b^\ell \}\rangle_{\partial I_n} \\ &= \left((v_N^\ell)', (\mathcal{I}u^\ell)'\right)_{I_n} - \langle (\mathcal{I}u^\ell)', \mathbf{n}(v_0^\ell - v_b^\ell)\rangle_{\partial I_n} \quad \ell = 1,2. \end{aligned} \tag{64}$$

From the definition of the interpolation and integration by parts, we obtain

$$\left((u^\ell - \mathcal{I}u^\ell)', (v_0^1)'\right)_{I_n} = -\left(u^\ell - \mathcal{I}u^\ell, (v_0^\ell)''\right)_{I_n} + \langle u^\ell - \mathcal{I}u^\ell, \mathbf{n}(v_0^\ell)'\rangle_{\partial I_n} = 0, \quad \ell = 1,2,$$

which implies that

$$\left((\mathcal{I}u^\ell)', (v_0^\ell)'\right)_{I_n} = \left((u^\ell)', (v_0^\ell)'\right)_{I_n}, \quad \ell = 1,2. \tag{65}$$

We infer from the equations (63),(64) and (65) that

$$\left(d_w(\mathcal{I}u^\ell), d_w v_N^\ell\right)_{I_n} = \left((u^\ell)', (v_0^\ell)'\right)_{I_n} - \langle (\mathcal{I}u^\ell)', \mathbf{n}(v_0^\ell - v_b^\ell)\rangle_{\partial I_n} \quad \ell = 1,2. \tag{66}$$

Summing the equation (66) over all mesh $I_n \in \mathcal{T}_h$, we find

$$\left(d_w(\mathcal{I}u^\ell), d_w v_N^\ell\right) = \left((u^\ell)', (v_0^\ell)'\right) - \langle (\mathcal{I}u^\ell)', \mathbf{n}(v_0^\ell - v_b^\ell)\rangle \quad \ell = 1,2. \tag{67}$$

Using again the integration by parts one can show

$$-\left((u^\ell)'', v_0^\ell\right)_{I_n} = \left((u^\ell)', (v_0^\ell)'\right)_{I_n} - \langle (u^\ell)', \mathbf{n} v_0^\ell\rangle_{\partial I_n} \quad \ell = 1,2.$$

Summing the above equation over all mesh $I_n \in \mathcal{T}_h$, we get

$$\left(((u^\ell)', (v_0^\ell)'\right) = -\left((u^\ell)'', v_0^\ell\right) + \langle (u^\ell)', \mathbf{n}(v_0^\ell - v_b^\ell)\rangle, \quad \ell = 1,2, \tag{68}$$

where we used the fact that $\langle (u^\ell)', \mathbf{n} v_b^\ell\rangle = 0, \quad \ell = 1,2$. Finally, by plugging the equation (68) into (67), we arrive at the desired result (59).

Lastly, the proof of the equation (62) is obvious. We complete the proof. □

Lemma 5.4. *Let $\mathcal{I}\boldsymbol{u}$ and $\boldsymbol{u}_N$ be the interpolation of the exact solution and the numerical solution of problem (1) and (25), respectively. Let $\rho := \mathcal{I}\boldsymbol{u} - \boldsymbol{u}_N$. Then we have the following error equation for ρ*

$$a(\rho, \boldsymbol{v}_N) = T(\boldsymbol{u}, \boldsymbol{v}_N), \quad \forall \boldsymbol{v}_N \in [S_N^0]^2, \tag{69}$$

where $T(\boldsymbol{u}, \boldsymbol{v}_N) := T_1(\boldsymbol{u}, \boldsymbol{v}_N) + T_2(\boldsymbol{u}, \boldsymbol{v}_N)$. Here, $T_1(\boldsymbol{u}, \boldsymbol{v}_N) = T_1(u^1, v_N^1) + T_1(u^2, v_N^2)$ with $T_1(u^\ell, v_N^\ell)$ and $T_2(\boldsymbol{u}, \boldsymbol{v}_N)$ are defined by (61) and (62), respectively.

Proof. Multiplying the equation (1) by test functions $\mathbf{v}_N \in [S_N^0]^2$ gives

$$-\varepsilon_1^2\Big((u^1)'', v_0^1\Big) + \Big(a_{11}u^1 + a_{12}u^2, v_0^1\Big) = \Big(g_1, v_0^1\Big), \tag{70}$$

$$-\varepsilon_2^2\Big((u^2)'', v_0^2\Big) + \Big(a_{21}u^1 + a_{22}u^2, v_0^2\Big) = \Big(g_2, v_0^2\Big). \tag{71}$$

Using the fact that $\mathcal{I}\mathbf{u}$ is continuous in Ω such that $s(\mathcal{I}u^\ell, v_N^\ell) = 0, \quad \ell = 1,2$, Lemma 5.3 and the above equations (70) and (71), we have

$$a(\mathcal{I}\mathbf{u}, \mathbf{v}_N) = a_1(\mathcal{I}\mathbf{u}, \mathbf{v}_N) + a_2(\mathcal{I}\mathbf{u}, \mathbf{v}_N) = \Big(\mathbf{g}, \mathbf{v}_N\Big) + T(\mathbf{u}, \mathbf{v}_N). \tag{72}$$

The desired equation (69) follows from subtracting (1) from the equation (72). Thus, the proof is now completed. □

Next, we perform the error estimate for the error $\mathbf{u} - \mathbf{u}_N$ in the $|||\cdot|||_\varepsilon$ norm defined by (32). We split the error into two parts as

$$\mathbf{u} - \mathbf{u}_N = (\mathbf{u} - \mathcal{I}\mathbf{u}) + (\mathcal{I}\mathbf{u} - \mathbf{u}_N) = \theta + \rho.$$

The following lemma will be useful in the error analysis.

Lemma 5.5. *Assume that $u^\ell \in H^{k+1}(\Omega)$. Then we have the following estimate*

$$\sum_{I_n \subset \Omega_s} \|(\theta^\ell)'\|^2_{L^2(\partial I_n)} \le \begin{cases} C\varepsilon_2^{-2}(N^{-1}\ln N)^{2k-1}, & s = 1,2,4,5, \\ C\varepsilon_2^{-2}N^{-2(k+1)}, & s = 3, \end{cases}$$

where $\theta^\ell = u^\ell - \mathcal{I}u^\ell$ for $\ell = 1,2$.

Proof. From the trace inequality (29), we can write

$$\|(\theta^\ell)'\|^2_{L^2(\partial I_n)} \le h_n^{-1}\|(\theta^\ell)'\|^2_{L^2(I_n)} + \|(\theta^\ell)'\|_{L^2(I_n)}\|(\theta^\ell)''\|_{L^2(I_n)}.$$

It remains to estimate $\|(\theta^\ell)'\|_{L^2(I_n)}$ and $\|(\theta^\ell)''\|_{L^2(I_n)}$, individually. From the estimate (49), one has

$$\begin{aligned} &\|(R^\ell - \mathcal{I}R^\ell)'\|_{L^2(\Omega)} \le CN^{-k}, \quad \ell = 1,2, \\ &\|(R^\ell - \mathcal{I}R^\ell)''\|_{L^2(\Omega)} \le CN^{-k+1}, \quad \ell = 1,2. \end{aligned} \tag{73}$$

With the help of the estimate (54) and (55) one can show that

$$\begin{aligned} &\|(L^\ell - \mathcal{I}L^\ell)'\|_{L^2(\Omega_3)} \le C\varepsilon_2^{-1/2}N^{-(k+1)}, \quad \ell = 1,2, \\ &\|(L^\ell - \mathcal{I}L^\ell)''\|_{L^2(\Omega_3)} \le C\varepsilon_2^{-3/2}N^{-(k+1)}, \quad \ell = 1,2, \\ &\|(L^\ell - \mathcal{I}L^\ell)'\|_{L^2(\Omega_s)} \le C\varepsilon_2^{-1/2}(N^{-1}\ln N)^{k}, \quad \ell = 1,2, \quad s = 1,2,4,5, \\ &\|(L^\ell - \mathcal{I}L^\ell)''\|_{L^2(\Omega_3)} \le C\varepsilon_2^{-3/2}(N^{-1}\ln N)^{k-1}, \quad \ell = 1,2, \quad s = 1,2,4,5. \end{aligned} \tag{74}$$

where the fact that $\varepsilon_2 N \le 1$ is used. From the above estimate and the triangle inequality, we can arrive at

$$\sum_{I_n \subset \Omega_s} \|(\theta^\ell)'\|_{L^2(I_n)} \le \begin{cases} C\varepsilon_2^{-1/2}(N^{-1}\ln N)^{k}, & s = 1,2,4,5, \\ C\varepsilon_2^{-1/2}N^{-k}(N^{-1} + \varepsilon_2^{1/2}), & s = 3, \end{cases} \tag{75}$$

and

$$\sum_{I_n \subset \Omega_s} \|(\theta^\ell)''\|_{L^2(I_n)} \le \begin{cases} C\varepsilon_2^{-3/2}(N^{-1}\ln N)^{k-1}, & s = 1,2,4,5, \\ C\varepsilon_2^{-3/2}N^{-k+1}(N^{-2} + \varepsilon_2^{3/2}), & s = 3. \end{cases}$$

The desired result follows from combining the above estimates. Thus, we complete the proof. □

Lemma 5.6. *Assume that $u^\ell \in H^{k+1}(\Omega)$ and the penalization parameter σ_n is given by (28). Then we have*

$$T(\boldsymbol{u}, \boldsymbol{v}_N) \leq C(N^{-1}\ln N)^k |||\boldsymbol{v}_N|||_\varepsilon, \tag{76}$$

where C is independent of N and ε_i, $i = 1, 2$.

Proof. It follows from the Cauchy-Schwarz inequality and Lemma 5.5 that for $\ell = 1, 2$

$$\begin{aligned}
|T_1(u^\ell, v_N^\ell)| &\leq \sum_{n=1}^{N} \varepsilon_\ell^2 |\langle (u^\ell - \mathcal{I}u^\ell)', (v_0^\ell - v_b^\ell)\mathbf{n}\rangle_{\partial I_n}| \\
&\leq \sum_{n=1}^{N} \varepsilon_\ell^2 \|(u^\ell - \mathcal{I}u^\ell)'\|_{L^2(\partial I_n)} \|v_0^\ell - v_b^\ell\|_{L^2(\partial I_n)} \\
&\leq \left\{ \sum_{n=1}^{N} \frac{\varepsilon_2^2}{\sigma_n} \|(u^\ell - \mathcal{I}u^\ell)'\|^2_{L^2(\partial I_n)} \right\}^{1/2} \left\{ \sum_{n=1}^{N} \sigma_n \|v_0^\ell - v_b^\ell\|^2_{L^2(\partial I_n)} \right\}^{1/2} \\
&\leq \left\{ \sum_{I_n \in \Omega\setminus\Omega_3} \frac{\varepsilon_2^2}{\sigma_n} \|(u^\ell - \mathcal{I}u^\ell)'\|^2_{L^2(\partial I_n)} + \sum_{I_n \in \Omega_3} \frac{\varepsilon_2^2}{\sigma_n} \|(u^\ell - \mathcal{I}u^\ell)'\|^2_{L^2(\partial I_n)} \right\}^{1/2} s^{1/2}(v_N^\ell, v_N^\ell) \\
&\leq C(N^{-1}\ln N)^k s^{1/2}(v_N^\ell, v_N^\ell).
\end{aligned}$$

As a result

$$|T_1(\mathbf{u}, \mathbf{v}_N)| \leq |T_1(u^1, v_N^1)| + |T_1(u^2, v_N^2)| \leq C(N^{-1}\ln N)^k |||\mathbf{v}_N|||_\varepsilon. \tag{77}$$

We next bound the term $T_2(\mathbf{u}, \mathbf{v}_N)$. We need to estimate $\|u^\ell - \mathcal{I}u^\ell\|$, $\ell = 1, 2$. Using the estimates (49)-(52) of Lemma 5.2 and the Cauchy-Schwarz inequality, we get for $\ell = 1, 2$,

$$\begin{aligned}
\|u^\ell - \mathcal{I}u^\ell\|_{L^2(\Omega)} &\leq \|R^\ell - \mathcal{I}R^\ell\|_{L^2(\Omega)} + \|L^\ell - \mathcal{I}L^\ell\|_{L^2(\Omega\setminus\Omega_3)} \\
&\quad + \|L^\ell\|_{L^2(\Omega_3)} + \|\mathcal{I}L^\ell\|_{L^2(\Omega_3)} \\
&\leq CN^{-(k+1)}[1 + \varepsilon_2^{1/2}(\ln N)^{k+1} + \varepsilon_2^{1/2} + N^{-1/2}] \\
&\leq CN^{-(k+1)}[1 + \varepsilon_2^{1/2}(\ln N)^{k+1}] \\
&\leq CN^{-(k+1)}.
\end{aligned} \tag{78}$$

The above estimate (78) and the Cauchy-Schwarz inequality yield the following estimates

$$\begin{aligned}
\left(a_{11}(\mathcal{I}u^1 - u^1), v_0^1\right) &\leq C\|u^1 - \mathcal{I}u^1\|\|v_0^1\| \leq CN^{-(k+1)}\|v_0^1\|, \\
\left(a_{21}(\mathcal{I}u^1 - u^1), v_0^2\right) &\leq C\|u^1 - \mathcal{I}u^1\|\|v_0^2\| \leq CN^{-(k+1)}\|v_0^2\|, \\
\left(a_{12}(\mathcal{I}u^2 - u^2), v_0^1\right) &\leq C\|u^2 - \mathcal{I}u^2\|\|v_0^1\| \leq CN^{-(k+1)}\|v_0^1\|, \\
\left(a_{22}(\mathcal{I}u^2 - u^2), v_0^1\right) &\leq C\|u^2 - \mathcal{I}u^2\|\|v_0^2\| \leq CN^{-(k+1)}\|v_0^2\|.
\end{aligned}$$

Combining the above estimates gives the bound for $T_2(\mathbf{u}, \mathbf{v}_N)$ as

$$|T_2(\mathbf{u}, \mathbf{v}_N)| \leq CN^{-(k+1)} |||\mathbf{v}_N|||_\varepsilon. \tag{79}$$

From the estimates (77) and (79), we have the desired result. Thus we complete the proof. □

In order to estimate the error between the analytical solution and the numerical solution obtained by the WG-FEM of the problem (1), we first derive the error estimate for the interpolation error θ in the energy-like norm $|||\cdot|||_\varepsilon$ in the following theorem.

Theorem 5.7. *Let $u^\ell \in H^{k+1}(\Omega)$, $\ell = 1, 2$ and the conditions of Lemma 5.2 hold. Then the following holds true*

$$|||\boldsymbol{u} - \mathcal{I}\boldsymbol{u}|||_\varepsilon \leq C(N^{-1}\ln N)^k, \tag{80}$$

where C is independent of N and $\varepsilon_i, i = 1, 2$.

Proof. Since $\theta^\ell = u^\ell - \mathcal{I}u^\ell$ is continuous on Ω, we get $s(\theta^\ell, \theta^\ell) = 0$ for $\ell = 1, 2$. Then the energy norm equals

$$|||\mathbf{u} - \mathcal{I}\mathbf{u}|||_\varepsilon^2 = \varepsilon_1^2\|(\theta^1)'\|^2 + \varepsilon_2^2\|(\theta^2)'\|^2 + \beta^2(\|\theta^1\|^2 + \|\theta^2\|^2) \tag{81}$$

In the light of the error estimate (75), we obtain

$$\begin{aligned} \varepsilon_2^2\|(\theta^\ell)'\|^2 &\leq \varepsilon_2^2\|(\theta^\ell)'\|^2_{L^2(\Omega\setminus\Omega_3)} + \varepsilon_2^2\|(\theta^\ell)'\|^2_{L^2(\Omega_3)} \\ &\leq (N^{-1}\ln N)^{2k} + N^{-2(k+1)} + \varepsilon_2 N^{-2k}, \end{aligned} \tag{82}$$

which together with (78) leads to the estimate (80)

$$|||\mathbf{u} - \mathcal{I}\mathbf{u}|||_\varepsilon \leq C(N^{-1}\ln N)^k,$$

which completes the proof. □

We next prove the error estimate for the discretization error $\rho = \mathcal{I}\mathbf{u} - \mathbf{u}_N$ in the energy-like norm.

Theorem 5.8. *Assume that $\boldsymbol{u} = (u^1, u^2)$, $u^\ell \in H^{k+1}(\Omega)$, $\ell = 1, 2$ is the exact solution and $\boldsymbol{u}_N \in [S_N^0]^2$ is the WG-FEM solution given by (25) on the uniform Shishkin mesh for the problem (1), respectively. Then the following estimate holds true*

$$|||\mathcal{I}\boldsymbol{u} - \boldsymbol{u}_N|||_\varepsilon \leq C(N^{-1}\ln N)^k,$$

where C is independent of N and $\varepsilon_i, i = 1, 2$.

Proof. With the help of Lemma 4.3, we have

$$a(\rho, \rho) \geq C|||\rho|||_\varepsilon. \tag{83}$$

Choosing $\mathbf{v}_N = \rho$ in the error equation (69) yields

$$a(\rho, \rho) = T(\mathbf{u}, \rho).$$

Using Lemma 5.6, we have

$$a(\rho, \rho) \leq C(N^{-1}\ln N)^k|||\rho|||_\varepsilon,$$

which together with (83) gives the desired result. Thus we complete the proof. □

Theorem 5.9. *Assume that $\boldsymbol{u} = (u^1, u^2)$, $u^\ell \in H^{k+1}(\Omega)$, $\ell = 1, 2$ is the exact solution and $\boldsymbol{u}_N \in [S_N^0]^2$ is the WG-FEM solution given by (25) on the uniform Shishkin mesh for the problem (1), respectively. Assume that $\varepsilon_2 N \leq C$. Then the following estimate holds true*

$$|||\boldsymbol{u} - \boldsymbol{u}_N|||_\varepsilon \leq C(N^{-1}\ln N)^k,$$

where C is independent of N and $\varepsilon_i, i = 1, 2$.

Proof. The triangle inequality and the conclusions of Theorem 5.7 and Theorem 5.8 imply the desired result. The proof is now completed. □

6. Numerical Experiments

In this section, various numerical examples are presented to verify computationally the theoretical findings in this paper. Let $e^N_{\varepsilon_1,\varepsilon_2} = \|\mathbf{u} - \mathbf{u}_N\|_\varepsilon$ denote the error between the exact solution $\mathbf{u}$ and the WG-FEM approximation $\mathbf{u}_N = (u^1_N, u^2_N) = \left(\{u^1_0, u^1_b\}, \{u^2_0, u^2_b\}\right)$ obtained by (25) on the Shishkin mesh with N number of interval.

If $\varepsilon_1 = 10^{-r}$ for $r = 3, 4, \ldots, 9$, we define $e^N_{\varepsilon_1} = \max\{e^N_{\varepsilon_1,1}, e^N_{\varepsilon_1,10^{-1}}, e^N_{\varepsilon_1,10^{-2}}, e^N_{\varepsilon_1,10^{-3}}, \ldots, e^N_{\varepsilon_1,10^{-r}}\}$. Then we calculated the uniform convergence error as $e^N = \max\{e^N_{10^{-3}}, e^N_{10^{-4}}, \ldots, e^N_{10^{-9}}\}$. We compute the orders of convergence (OC) using the formula

$$r^N = \frac{\ln(e_{N/2}/e_N)}{\ln(2\ln(N/2)) - \ln(\ln(N))}. \tag{84}$$

We start with verifying the OC rate of the errors in the energy norm $|||\cdot|||_\varepsilon$ defined by (32). We also provide the convergence results of the error e^N in the discrete L^2- norm defined as

$$\|\mathbf{u} - \mathbf{u}_0\|_{L^2(\mathcal{T}_N)} := \left\{\sum_{n=1}^{N} \left(\|u^1 - u^1_0\|^2_{L^2(I_n)} + \|u^2 - u^2_0\|^2_{L^2(I_n)}\right)\right\}^{1/2},$$

and the discrete $L^\infty-$ norm defined by

$$\|\mathbf{u} - \mathbf{u}_b\|_{L^\infty(\mathcal{T}_N)} := \max_{0\le n\le N} \left(|u^1(x_n) - u^1_b(x_n)| + |u^2(x_n) - u^2_b(x_n)|\right).$$

Example 6.1. *Consider the following coupled system of reaction-diffusion problem*

$$\begin{cases} -\mathcal{E}\boldsymbol{u}'' + \boldsymbol{A}\boldsymbol{u} = \boldsymbol{g} \quad in \quad \Omega = (0,1), \\ \boldsymbol{u}(0) = \boldsymbol{0}, \quad \boldsymbol{u}(1) = \boldsymbol{0} \end{cases} \tag{85}$$

where $\mathcal{E} = diag(\varepsilon_1^2, \varepsilon_2^2)$ *with* $0 < \varepsilon_1 \le \varepsilon_2 << 1$, $\boldsymbol{g} = (g_1, g_2)^T$, $\boldsymbol{A} = \begin{bmatrix} 2 & -1 \\ -1 & 2 \end{bmatrix}$ *and* g_1, g_2 *are chosen such that*

$$u^1(x) = \frac{e^{-x/\varepsilon_1} + e^{-(1-x)/\varepsilon_1}}{1 + e^{-1/\varepsilon_1}} + \frac{e^{-x/\varepsilon_2} + e^{-(1-x)/\varepsilon_2}}{1 + e^{-1/\varepsilon_2}} - 2,$$
$$u^2(x) = \frac{e^{-x/\varepsilon_2} + e^{-(1-x)/\varepsilon_2}}{1 + e^{-1/\varepsilon_2}} - 1,$$

is the exact solution $\boldsymbol{u}(x) = (u^1(x), u^2(x))$ *of the system of reaction-diffusion problem (85). We know that the solution has exponential layers of width* $O(\varepsilon_2|\ln\varepsilon_2|)$ *at* $x = 0$ *and* $x = 1$*, while only* $u^1(x)$ *has an additional sublayer of width* $O(\varepsilon_1|\ln\varepsilon_1|)$*. The conditions (2) and (3) are satisfied for any* $\beta \in (0,1)$ *and we take* $\beta = 0.95$ *in the construction of Shishkin mesh for this problem.*

In Table 1, we report the errors and the OC in the energy norm defined by (32) for $N = 16, 32, 64, 128, 256, 512, 1024$ and $\varepsilon_1 \in \{10^{-3}, 10^{-4}, \ldots, 10^{-9}\}$ with $\varepsilon_2 \in \{1, 10^{-1}, \ldots, 10^{-9}\}$. We observe from Table 1 that the method exhibits $k-$th order convergence and the rate of convergence is $O((N^{-1}\ln N)^k)$ in the energy-like norm (32). Note that the errors do not depend on the perturbation parameters ε_1 and ε_2. These results are in good agreement with the theoretical results of Theorem 5.9. Figure 2 has a log-log plot of numerical errors in $|||\mathbf{u} - \mathbf{u}_N|||_\varepsilon$, $\|\mathbf{u} - \mathbf{u}_N\|_{L^2(\mathcal{T}_N)}$ and $\|\mathbf{u} - \mathbf{u}_b\|_{L^\infty(\mathcal{T}_N)}$ with $\varepsilon_1 = 10^{-8}, \varepsilon_2 = 10^{-6}$ for the WG-FEM in Example 6.1. We observe that the rate of convergence in the $|||\cdot|||_\varepsilon$- norm is $O((N^{-1}\ln N)^k)$. Again, these results match the theory we have developed in Theorem 5.9. Figure 2 shows that the WG-FEM approximation (25) seems to have the optimal convergence rate of $O(N^{-(k+1)})$ in the L^2- norm and the convergence rate of $O((N^{-1}\ln N)^{2k})$ in the discrete L^∞-norm.

$\varepsilon_1/k=1$	N						
	16	32	64	128	256	512	1024
10^{-3}	1.0674E-01	5.3675E-02	2.7001E-02	1.3617E-02	6.8906E-03	3.4992E-03	1.7730E-03
10^{-4}	1.1218E-01	5.6423E-02	2.7001E-02	1.4144E-02	7.0780E-03	3.5425E-03	1.7735E-03
10^{-5}	1.1127E-01	5.6739E-02	2.8422E-02	1.4219E-02	7.1113E-03	3.5561E-03	1.7783E-03
10^{-6}	1.1284E-01	5.6771E-02	2.8438E-02	1.4227E-02	7.1148E-03	3.5575E-03	1.7788E-03
10^{-7}	1.1284E-01	5.6774E-02	2.8440E-02	1.4228E-02	7.1151E-03	3.5577E-03	1.7788E-03
10^{-8}	1.1284E-01	5.6774E-02	2.8440E-02	1.4228E-02	7.1152E-03	3.5577E-03	1.7788E-03
10^{-9}	1.1284E-01	5.6774E-02	2.8440E-02	1.4228E-02	7.1152E-03	3.5577E-03	1.7788E-03
e^N	1.1284E-01	5.6774E-02	2.8440E-02	1.4228E-02	7.1152E-03	3.5577E-03	1.7888E-03
r^N	-	1.4615	1.3532	1.2849	1.2383	1.2046	1.1792
$\varepsilon_1/k=2$							
10^{-3}	2.0122E-02	9.0128E-03	3.4633E-03	1.1885E-03	3.8181E-04	1.1833E-04	3.5893E-05
10^{-4}	3.8917E-02	1.9112E-02	7.7816E-03	2.7863E-03	9.1343E-04	2.8528E-04	8.6407E-05
10^{-5}	4.2500E-02	2.1289E-02	8.8877E-03	3.2331E-03	1.0811E-03	3.4433E-04	1.0633E-04
10^{-6}	4.2881E-02	2.1522E-02	9.0038E-03	3.2821E-03	1.0997E-03	3.5095E-04	1.0859E-04
10^{-7}	4.2919E-02	2.1546E-02	9.0156E-03	3.2870E-03	1.1016E-03	3.5162E-04	1.0882E-04
10^{-8}	4.2923E-02	2.1548E-02	9.0167E-03	3.2875E-03	1.1018E-03	3.5169E-04	1.0884E-04
10^{-9}	4.2924E-02	2.1549E-02	9.0168E-03	3.2876E-03	1.1018E-03	3.5170E-04	1.0885E-04
e^N	4.2924E-02	2.1549E-02	9.0168E-03	3.2876E-03	1.1018E-03	3.5170E-04	1.0885E-04
r^N	-	1.4661	1.7055	1.8718	1.9534	1.9847	1.9952
$\varepsilon_1/k=3$							
10^{-3}	8.9467E-03	3.1909E-03	8.8195E-04	1.9720E-04	3.8402E-05	6.8842E-06	1.1803E-06
10^{-4}	1.9784E-02	7.5587E-03	2.1392E-03	4.7806E-04	9.1942E-05	1.4030E-05	1.7289E-06
10^{-5}	2.2213E-02	8.7373E-03	2.5459E-03	5.8507E-04	1.1557E-04	1.8078E-05	2.2691E-06
10^{-6}	2.2475E-02	8.8662E-03	2.5911E-03	5.9716E-04	1.1828E-04	1.8550E-05	2.3340E-06
10^{-7}	2.2501E-02	8.8792E-03	2.5957E-03	5.9838E-04	1.1856E-04	1.8598E-05	2.3406E-06
10^{-8}	2.2504E-02	8.8805E-03	2.5961E-03	5.9851E-04	1.1859E-04	1.8603E-05	2.3413E-06
10^{-9}	2.2504E-02	8.8807E-03	2.5962E-03	5.9852E-04	1.1859E-04	1.8604E-05	2.3415E-06
e^N	2.2504E-02	8.8807E-03	2.5962E-03	5.9852E-04	1.1859E-04	1.8604E-05	2.3415E-06
r^N	-	1.97837	2.4075	2.7223	2.8926	3.2193	3.5261

Table 1: History of convergence of the WG-FEM in the $|||\cdot|||_\varepsilon$ norm for Example 6.1

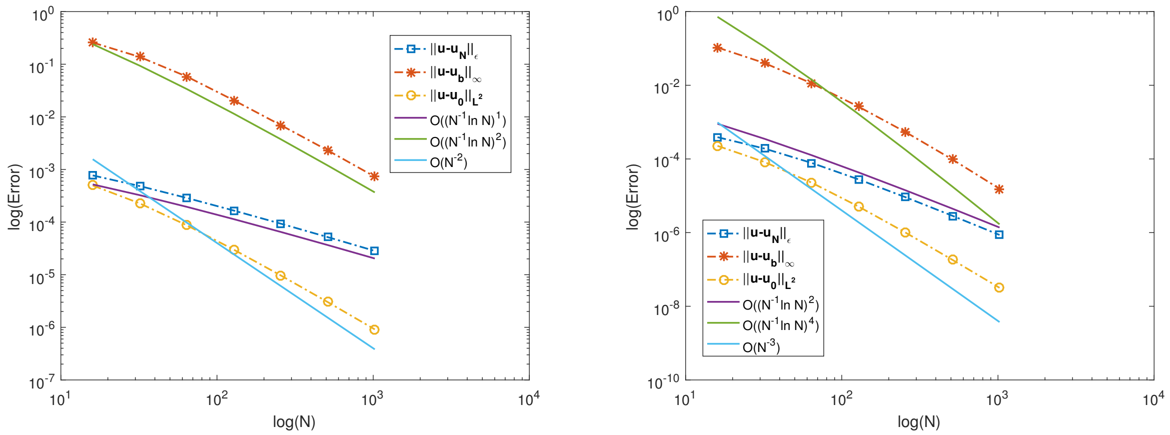

(a) $\mathbb{P}^1$ element (b) $\mathbb{P}^2$ element

Figure 2: Convergence curve of error in Example 6.1 with $\varepsilon_1 = 10^{-8}$ and $\varepsilon_2 = 10^{-6}$ using (2(a)) linear and (2(b)) quadratic element functions.

Example 6.2. *This example is taken from [17]. Consider the following coupled system of variable coefficient reaction-diffusion problem.*

$$\begin{cases} -\mathcal{E}\boldsymbol{u}'' + \boldsymbol{A}\boldsymbol{u} = \boldsymbol{g} \quad in \quad \Omega = (0,1), \\ \boldsymbol{u}(0) = \boldsymbol{0}, \quad \boldsymbol{u}(1) = \boldsymbol{0} \end{cases}$$

where $\mathcal{E} = diag(\varepsilon_1^2, \varepsilon_2^2)$ *with* $0 < \varepsilon_1 \le \varepsilon_2 << 1, \quad \boldsymbol{g} = (2e^x, 10x+1)^T$ *and*

$$\boldsymbol{A} = \begin{bmatrix} 2(x+1)^2 & -(1+x^3) \\ -2\cos(\frac{\pi x}{4}) & 3e^{1-x} \end{bmatrix}.$$

The conditions (2) and (3) are satisfied for any $\beta \in (0,1)$ for this problem. The exact solution to this problem is not available. Therefore, we estimate the errors by using the following double mesh principle. Let $\mathbf{u}_N$ be the solution of the WG finite element scheme (25) on the original Shishkin mesh and $\mathbf{u}_{2N} = (u_{2N}^1, u_{2N}^2) = (\{u_{20}^1, u_{2b}^1\}, \{u_{20}^2, u_{20}^2\})$ be the WG solution on the mesh obtained by combining the mesh points of the original mesh and its uniformly bisection points, i.e.,

$$x_{2n} = x_n, \quad n = 0, \dots, N, \quad x_{2n+1} = \frac{x_n + x_{n+1}}{2}, \quad n = 0, \dots, N-1. \tag{86}$$

We estimate the uniform error by

$$e^N := \max_S |||\mathbf{u}_N - \mathbf{u}_{2N}|||_\varepsilon,$$

where the singular perturbation parameters are evaluated on the set $S = \{(\varepsilon_1, \varepsilon_2) : \varepsilon_2 = 1, 10^{-1}, \dots, 10^{-9}, \varepsilon_1 = 10^{-3}, \dots, 10^{-9}\}$. The rates of convergence r^N are computed by the standard formula (84).

In Figure 3, we display the numerical solutions of Example 6.2 obtained by WG-FEM approximation (25) using linear element functions on Shishkin meshes with $N = 32$ number of elements for different perturbation parameters $(\varepsilon_1, \varepsilon_2) = (10^{-2}, 10^{-1})$ and $(\varepsilon_1, \varepsilon_2) = (10^{-6}, 10^{-4})$. We observe that there exist two boundary layers near $x = 0$ and $x = 1$ whereas only $u^1(x)$ has an additional sublayer of width $O(\varepsilon_1 |\ln \varepsilon_1|)$.

Table 2 presents the computed numerical values of $e_{\varepsilon_1}^N$ for $N = 16, 32, 64, 128, 256, 1024$ and $\varepsilon_1 \in \{10^{-3}, \dots, 10^{-9}\}$ for Example 6.2. We obtain the maximum value in each column and compute the OC in the last two rows,respectively for each element functions $k = 1, 2.3$. Figure 4 has a log-log plot of numerical errors in $|||\mathbf{u}_N - \mathbf{u}_{2N}|||_\varepsilon, \|\mathbf{u}_0 - \mathbf{u}_{20}\|_{L^2(\mathcal{T}_N)} = \left\{\sum_{n=1}^N \left(\|u_0^1 - u_{20}^1\|_{L^2(I_n)}^2 + \|u_0^2 - u_{20}^2\|_{L^2(I_n)}^2\right)\right\}^{1/2}$ and $\|\mathbf{u}_b - \mathbf{u}_{2b}\|_{L^\infty(\mathcal{T}_N)} :=$

$\varepsilon_1/k=1$	N						
	16	32	64	128	256	512	1024
10^{-3}	2.3946E+00	1.6284E+00	1.0156E+00	6.0149E-01	3.4556E-01	1.9473E-01	1.0824E-01
10^{-4}	2.3940E+00	1.6281E+00	1.0154E+00	6.0138E-01	3.4550E-01	1.9469E-01	1.0823E-01
10^{-5}	2.3939E+00	1.6280E+00	1.0154E+00	6.0137E-01	3.4550E-01	1.9469E-01	1.0822E-01
10^{-6}	2.3939E+00	1.6280E+00	1.0154E+00	6.0137E-01	3.4550E-01	1.9469E-01	1.0822E-01
10^{-7}	2.3939E+00	1.6280E+00	1.0154E+00	6.0137E-01	3.4550E-01	1.9469E-01	1.0822E-01
10^{-8}	2.3939E+00	1.6280E+00	1.0154E+00	6.0137E-01	3.4550E-01	1.9469E-01	1.0822E-01
10^{-9}	2.3939E+00	1.6280E+00	1.0154E+00	6.0137E-01	3.4550E-01	1.9470E-01	1.0859E-01
e^N	2.3946E+00	1.6284E+00	1.0156E+00	6.0149E-01	3.4556E-01	1.9473E-01	1.0859e-01
r^N	-	0.82	0.92	0.97	0.99	1.00	1.00
$\varepsilon_1/k=2$							
10^{-3}	1.1471e+00	5.6576e-01	2.3036e-01	8.2704e-02	2.7558e-02	8.7806e-03	2.7162e-03
10^{-4}	1.1469e+00	5.6574e-01	2.3038e-01	8.2715e-02	2.7562e-02	8.7819e-03	2.7166e-03
10^{-5}	1.1469e+00	5.6573e-01	2.3038e-01	8.2716e-02	2.7563e-02	8.7821e-03	2.7166e-03
10^{-6}	1.1469e+00	5.6573e-01	2.3038e-01	8.2716e-02	2.7563e-02	8.7821e-03	2.7167e-03
10^{-7}	1.1469e+00	5.6573e-01	2.3038e-01	8.2716e-02	2.7563e-02	8.7820e-03	2.7180e-03
10^{-8}	1.1469e+00	5.6573e-01	2.3038e-01	8.2716e-02	2.7563e-02	8.7858e-03	2.7180e-03
10^{-9}	1.1469e+00	5.6573e-01	2.3038e-01	8.2714e-02	2.7600e-02	8.7880e-03	2.7180e-03
e^N	1.1471e+00	5.6576e-01	2.3038e-01	8.2716e-02	2.7600e-02	8.7880e-03	2.7180e-03
r^N	-	1.5039	1.7588	1.9004	1.9613	1.9891	1.9965
$\varepsilon_1/k=3$							
10^{-3}	5.2331e-01	3.2797e-01	1.7145e-01	6.4712e-02	1.7388e-02	3.6364e-03	6.6128e-04
10^{-4}	5.2296e-01	3.2782e-01	1.7146e-01	6.4714e-02	1.7386e-02	3.6357e-03	6.6111e-04
10^{-5}	5.2296e-01	3.2780e-01	1.7146e-01	6.4714e-02	1.7386e-02	3.6356e-03	6.6110e-04
10^{-6}	5.2296e-01	3.2780e-01	1.7146e-01	6.4714e-02	1.7386e-02	3.6357e-03	6.6115e-04
10^{-7}	5.2296e-01	3.2780e-01	1.7146e-01	6.4714e-02	1.7386e-02	3.6358e-03	6.6299e-04
10^{-8}	5.2296e-01	3.2780e-01	1.7146e-01	6.4714e-02	1.7386e-02	3.6422e-03	6.7938e-04
10^{-9}	5.2297e-01	3.2781e-01	1.7146e-01	6.4713e-02	1.7406e-02	3.8158e-03	6.8425e-04
e^N	5.2331e-01	3.2797e-01	1.7146e-01	6.4714e-02	1.7406e-02	3.8158e-03	6.84250e-04
r^N	-	0.9941	1.2697	1.8078	2.3465	2.6377	2.9238

Table 2: History of convergence of the WG-FEM in the $|||\mathbf{u}_N - \mathbf{u}_{2N}|||_\varepsilon$ norm for Example 6.2

$\max_{0\le n\le N}\left(|u_b^1(x_n) - u_{2b}^1(x_n)| + |u_b^2(x_n) - u_{2b}^2(x_n)|\right)$ with $\varepsilon_1 = 10^{-8}, \varepsilon_2 = 10^{-6}$ for the WG-FEM in Example 6.2. We observe that the rate of convergence in the $|||\cdot|||_\varepsilon$- norm is $O((N^{-1}\ln N)^k)$. Again, these results support the theory in Theorem 5.9. Figure 4 shows that the WG-FEM approximation (25) has the optimal convergence rate of $O(N^{-(k+1)})$ in the L^2-norm and the convergence rate of $O((N^{-1}\ln N)^{2k})$ in the discrete L^∞-norm as in Example 6.2.

We compare the numerical errors of the classical FEM, the discontinuous Galerkin finite element method (DGFEM) and the WG-FEM for Example 6.2 in Table 3. In the computation, we estimate the uniform error by

$$e^{\mathrm{N}} := \max_{\varepsilon_1,\varepsilon_2=1,10^{-1},\ldots,10^{-12}} \left\|\mathrm{u}_{\mathrm{N}}^{\varepsilon_1,\varepsilon_2} - \mathrm{u}_{8\,\mathrm{N}}^{\varepsilon_1,\varepsilon_2}\right\|,$$

where $\mathrm{u}_{\mathrm{N}}^{\varepsilon_1,\varepsilon_2}$ denotes the numerical approximation depends on N, ε_1 and ε_2, and $\mathrm{u}_{8\,\mathrm{N}}^{\varepsilon_1,\varepsilon_2}$ is the approximation solution of the FEM or the DGFEM or the WG-FEM on a mesh obtained by bisecting the original mesh three times, i.e., a mesh that is eight times finer. We see that the errors computed by the WG-FEM is very close to those computed by FEM and superior to the errors computed by DGFEM.

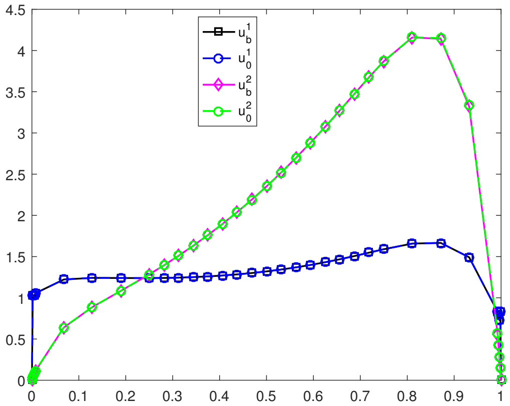

(a) The WG-FEM solution with $(\varepsilon_1, \varepsilon_2) = (10^{-3}, 10^{-1})$

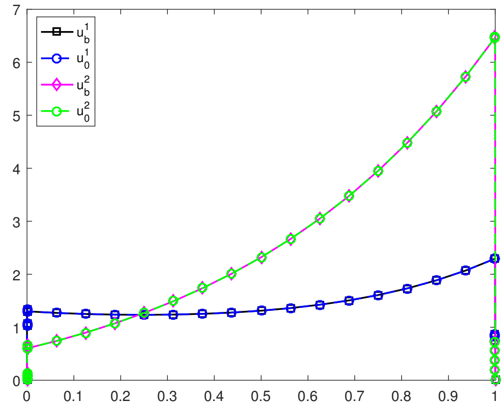

(b) The WG-FEM solution with $(\varepsilon_1, \varepsilon_2) = (10^{-6}, 10^{-4})$

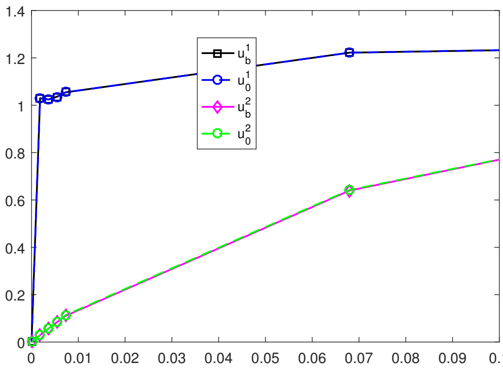

(c) The plot (3(a)) zoomed in on the interval $(0, 0.1)$.

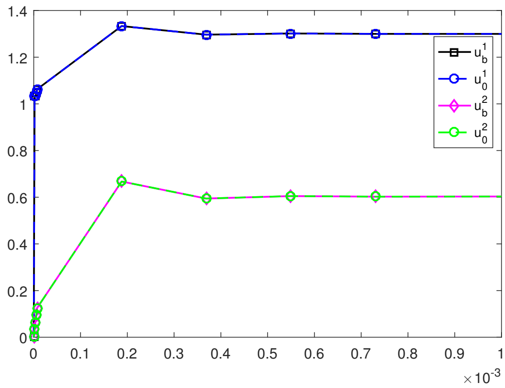

(d) The plot (3(b)) zoomed in on the interval $(0, 0.001)$.

Figure 3: The WG-FEM solution $\mathbf{u}_N = \left(\{u_0^1, u_b^1\}, \{u_0^2, u_b^2\}\right)$ in Example 6.2 using $\mathbb{P}^1$ element with $N = 32$ and different perturbation parameters $(\varepsilon_1, \varepsilon_2) = (10^{-3}, 10^{-1})$ in Figure 3(a) and $(\varepsilon_1, \varepsilon_2) = (10^{-6}, 10^{-4})$ in Figure 3(b). Figure 3(c) and Figure 3(d) demonstrate zoomed in of the plots on the finer interval near the left boundary.

N	FEM [14]	DGFEM [24]	The WG-FEM
128	4.3421e-01	6.0135e-01	4.3799e-01
256	2.5643e-01	3.4844e-01	2.5931e-01
512	1.4271e-01	1.8062e-01	1.4678e-01
1024	8.1378e-02	8.7835e-02	8.1443e-02

Table 3: Comparison of the numerical errors of FEM, DFEM and the WG-FEM for Example 6.2 using $\mathbb{P}_1$ elements.

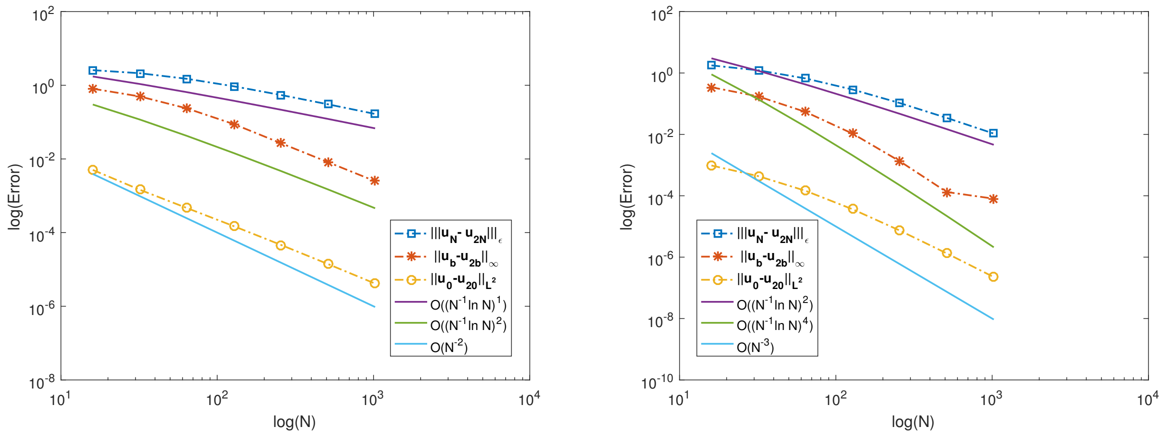

(a) $\mathbb{P}^1$ element

(b) $\mathbb{P}^2$ element

Figure 4: Convergence curve of error in Example 6.2 with $\varepsilon_1 = 10^{-8}$ and $\varepsilon_2 = 10^{-6}$ using (4(a)) linear and (4(b)) quadratic element functions.

7. Conclusion

In this work, we have developed the WG-FEM for a coupled system of singularly perturbed reaction-diffusion problems. Theoretically and numerically, we have proved uniformly convergent error estimates of order $O(N^{-1}\ln N)^k$ in the $(\varepsilon_1, \varepsilon_2)$-dependent WG energy norm on Shishkin mesh, where k is the order of polynomials used in the approximation space. The proposed method in this paper can be extended to a coupled system of singularly perturbed reaction-diffusion problems in higher dimensional. The main difficulty is to find a *priori* bounds on the derivatives of the solutions when each perturbation parameter in the system has a different magnitude. We will investigate this direction in ongoing work.

References

[1] A. Al-Taweel, S. Hussain, X. Wang, and B. Jones, *A P0 – P0 weak Galerkin finite element method for solving singularly perturbed reaction-diffusion problems*, Numer. Methods Partial Differ. Equtions, 36 (2020), pp. 213–227.

[2] N. Bakhvalov, *The optimization of methods of solving boundary value problems with a boundary layer*, U.S.S.R Comput. Math. Math. Phys., 9 (1969), pp. 139–166.

[3] S. Chen, Y. Wang, and X. Wu, *Rational spectral collocation method for a coupled system of singularly perturbed boundary value problems*, J. Comput. Math., (2011), pp. 458–473.

[4] C. Clavero, J. Gracia, and F. Lisbona, *An almost third order finite difference scheme for singularly perturbed reaction–diffusion systems*, J. Comput. Appl. Math., 234 (2010), pp. 2501–2515.

[5] M. Cui and S. Zhang, *On the uniform convergence of the weak Galerkin finite element method for a singularly-perturbed biharmonic equation*, J. Sci. Comput., 82 (2020), p. 5.

[6] P. Das and S. Natesan, *A uniformly convergent hybrid scheme for singularly perturbed system of reaction-diffusion robin type boundary-value problems*, J. Appl. Math. Comput., 41 (2013), pp. 447–471.

[7] P. Das and S. Natesan, *Error estimate using mesh equidistribution technique for singularly perturbed system of reaction-diffusion boundary-value problems*, Appl. Math. Comput., 249 (2014), p. 265–277.

[8] R. Lin and M. Stynes, *Numerical solution of systems of singularly perturbed differential equations*, Comput. Methods Appl. Math., 9(2) (2009), p. 6165–191.

[9] ———, *A balanced finite element method for a system of singularly perturbed reaction-diffusion two-point boundary value problems*, Numer. Algor., 70(4) (2015), p. 691–707.

[10] R. Lin, X. Ye, S.Zhang, and P. Zhu, *A weak Galerkin finite element method for singularly perturbed convection-diffusion–reaction problems*, SIAM J. Numer. Anal., 56(3) (2018), pp. 1482—1497.

[11] T. Linss, *Layer–adapted meshes for one–dimensional reaction–convection–diffusion problems*, J. Numer. Math., 12(3) (2004), pp. 193–205.

[12] T. Linss, *Layer-adapted meshes for reaction-convection-diffusion problems*, Springer, 2009.

[13] T. Linss and N. Madden, *Accurate solution of a system of coupled singularly perturbed reaction-diffusion equations*, Computing, 73 (2004), p. 121–133.

[14] ———, *A finite element analysis of a coupled system of singularly perturbed reaction–diffusion equations*, Appl. Math. Comput., 148 (2004), p. 869–880.

[15] ———, *Layer-adapted meshes for a linear system of coupled singularly perturbed reaction–diffusion problems*, IMA J. Numer. Anal., 29 (2009), pp. 109–125.

[16] N. Madden and M. Stynes, *A uniformly convergent numerical method for a coupled system of two singularly perturbed linear reaction-diffusion problems*, IMA J. Numer. Anal., 23(4) (2003), p. 627–644.

[17] S. Matthwes, E. O'Riordan, and G. Shishkin, *A numerical method for a system of singularly perturbed reaction–diffusion equations*, J. Comput. Appl. Math., 145 (2002), pp. 151–166.

[18] J. J. Miller, E. O'riordan, and G. I. Shishkin, *Fitted numerical methods for singular perturbation problems: error estimates in the maximum norm for linear problems in one and two dimensions*, World scientific, 1996.

[19] L. Mu, J. Wang, X. Ye, and S. Zhao, *A weak Galerkin finite element method for the Maxwell equations*, J. Sci. Comput., 65 (2015), pp. 363–386.

[20] ———, *A new weak Galerkin finite element method for elliptic interface problems*, J. Comput. Phys., 325 (2016), pp. 157–173.

[21] S. Natesan and B. Deb, *A robust computational method for singularly perturbed coupled system of reaction-diffusion boundary-value problems*, Appl. Math. Comput., 188 (2007), p. 353–364.

[22] H.-G. Roos, M. Stynes, and L. Tobiska, *Robust Numerical Methods for Singularly Perturbed Differential Equations.*, Springer, Berlin, Heidelberg., Berlin, 2008.

[23] G. Shishkin, *Mesh approximation of singularly perturbed boundary-value problems for systems of elliptic and parabolic equations*, Comput. Math. Math. Phys., 35 (1995), p. 429–446.

[24] G. Singh and S. Natesan, *A uniformly convergent numerical scheme for a coupled system of singularly perturbed reaction-diffusion equations*, Numer. Funct. Anal. Optim., 41 (2020), pp. 1172–1189.

[25] S. Toprakseven, A weak Galerkin finite element method for time fractional reaction-diffusion-convection problems with variable coefficients, Appl. Numer. Math., 168 (2021), pp. 1–12.

[26] Ş. Toprakseven, *Optimal order uniform convergence in energy and balanced norms of weak Galerkin finite element method on bakhvalov-type meshes for nonlinear singularly perturbed problems*, Comput. Appl. Math, 41 (2022), p. 377.

[27] S. Toprakseven, *Superconvergence of a modified weak Galerkin method for singularly perturbed two-point elliptic boundary-value problems*, Calcolo, 59 (2022), pp. 1–35.

[28] Ş. Toprakseven, *A weak Galerkin finite element method on temporal graded meshes for the multi-term time fractional diffusion equations*, Comput. Math. Appl, 128 (2022), pp. 108–120.

[29] S. Toprakseven and P. Zhu, *Uniform convergent modified weak Galerkin method for convection-dominated two-point boundary value problems*, Turkish J. Math., 45 (2021), pp. 2703–2730.

[30] Ş. Toprakseven and P. Zhu, *Error analysis of a weak Galerkin finite element method for two-parameter singularly perturbed differential equations in the energy and balanced norms*, Appl. Math. Comput., 441 (2023), p. 127683.

[31] L. Tosbika, *Analysis of a new stabilized higher order finite element method for advection-diffusion equations*, . Comput. Methods Appl. Mech. Engrg., 196 (1-3) (2006), p. 538–550.

[32] J. Wang and X. Ye, *A weak Galerkin finite element method for second-order elliptic problems*, J. Comput. Appl. Math., 241 (2013), p. 103–115.

[33] ———, *A weak Galerkin finite element method for the Stokes equations*, Adv. Comput. Math., 42 (2016), p. 155–174.

[34] J. Zhang and X. Liu, *Uniform convergence of a weak Galerkin finite element method on shishkin mesh for singularly perturbed convection-diffusion problems in 2D*, Appl. Math. Comput., 432 (2022), p. 127346.

[35] J. Zhang and X. Liu, *Uniform convergence of a weak Galerkin method for singularly perturbed convection–diffusion problems*, Math. Comput. Simulation, 200 (2022), pp. 393–403.

[36] P. Zhu and S. Xie, *A uniformly convergent weak Galerkin finite element method on Shishkin mesh for 1d convection–diffusion problem*, J. Sci. Comput., 85 (2020), p. 34.